



Universität Hamburg
DER FORSCHUNG | DER LEHRE | DER BILDUNG

FAKULTÄT
FÜR WIRTSCHAFTS- UND
SOZIALWISSENSCHAFTEN

Replacing temperature targets by subsidiary targets: How accurate are they? – Overshooting vs. economic losses

Lukas Stein
Mohammad M. Khabbazan
Hermann Held

WiSo-HH Working Paper Series
Working Paper No. 57
March 2020



WiSo-HH Working Paper Series
Working Paper No. 57
March 2020

Replacing temperature targets by subsidiary targets: How accurate are they? – Overshooting vs. economic losses

Lukas Stein, University of Hamburg
Mohammad M. Khabbazan, University of Hamburg
Hermann Held, University of Hamburg

ISSN 2196-8128

Font used: „TheSans UHH“ / LucasFonts

Die Working Paper Series bieten Forscherinnen und Forschern, die an Projekten in Federführung oder mit der Beteiligung der Fakultät für Wirtschafts- und Sozialwissenschaften der Universität Hamburg tätig sind, die Möglichkeit zur digitalen Publikation ihrer Forschungsergebnisse. Die Reihe erscheint in unregelmäßiger Reihenfolge.

Jede Nummer erscheint in digitaler Version unter
<https://www.wiso.uni-hamburg.de/de/forschung/working-paper-series/>

Kontakt:

WiSo-Forschungslabor
Von-Melle-Park 5
20146 Hamburg
E-Mail: experiments@wiso.uni-hamburg.de
Web: <http://www.wiso.uni-hamburg.de/forschung/forschungslabor/home/>



Replacing temperature targets by subsidiary targets: How accurate are they? – Overshooting vs. economic losses

Lukas Stein^{*}, Mohammad M. Khabbazan^{*,**}, and Hermann Held^{*,**}

^{*}Research Unit Sustainability and Global Change

^{**}Center for Earth System Research and Sustainability

Universität Hamburg, Grindelberg 5, 20144 Hamburg, Germany

Correspondence to: Hermann Held (hermann.held@uni-hamburg.de)

Author contributions. L.S. performed all numerical and analytical work, prepared the graphs, and wrote most of the manuscript. H.H. suggested the concept of “internal targets” and thereby triggered this work. He also contributed to the writing of this manuscript and triggered the analytic approach. M.M.K. suggested analyzing the time-limited concentration target.

Competing interests. There are not competing interests present.

- 5 *Acknowledgements.* We would like to thank the cluster of excellence “Integrated Climate System Analysis and Prediction” (CliSAP) of Universität Hamburg for the provided funding (DFG grant EXC177). Particularly L.S. and M.M.K. were funded by CliSAP.

Replacing temperature targets by subsidiary targets: How accurate are they? – Overshooting vs. economic losses

Abstract. This article investigates the trade-off between increasing welfare losses and increasing peak-warming if a temperature target is reformulated as a subsidiary concentration or cumulative emissions target. We apply a welfare maximizing integrated assessment model for a deterministic cost-effectiveness analysis to identify the associated costs of a certain climate target. We find that the use of subsidiary targets, a common practice in integrated climate modeling, increases losses by at least 12% for time-limited concentration targets that allow for a peak before concentration stabilizes. For all-time concentration targets we find that losses increase at least by 50%. Under all-time cumulative emissions targets losses rise by at least 20%. If the subsidiary all-time targets are forced to have equal cost as their parental maximum-warming target, all-time cumulative emissions (concentration) targets overshoot by more than 0.1°C (0.2°C). Generally, among the investigated subsidiary targets, we find all-time cumulative emissions targets and time-limited concentration targets to behave most similar to the parental temperature targets.

1 Introduction

It is common practice in the integrated assessment modeling community on climate change to de-couple the economic optimization from the explicit calculation of a temperature or even radiative forcing IPCC WGIII (2014, Ch. 6, p. 428). Subsidiary cumulative emission or concentration targets are being used instead of the internationally agreed temperature targets (COP21, 2015). The subsidiary targets are based on the finding that peak warming linearly relates to the all-time cumulative emissions (IPCC WGI, 2013, Fig. SPM.10) or that 450 ppmvCO₂eq leads to 2°C warming (IPCC WGIII, 2014, SPM 4.1). The subsidiary targets are chosen such that their “parental” temperature target is not transgressed. When constraining integrated assessment models (IAMs) with those subsidiary targets, in effect two targets have to be complied with: the explicit subsidiary and its implicit “parental” target.

Hence, models that use subsidiary targets do not calculate the cost of a single target but of two targets. In a welfare maximizing IAM, applying an additional constraint by construction causes welfare losses because the solution space is narrowed (e.g. Held (2013)). In last consequence, the resulting welfare losses of the “parental” target are overestimated.

Vice versa, subsidiary targets with equal welfare losses as their “parental” target can be applied. They however, lead to a transgression of the “parental” target. Appendix section A briefly explains the mechanism of welfare loss once a subsidiary target has been put in operation.

It is the aim of this work to introduce above construction of subsidiary targets, then, to infer the numerical subsidiary counterparts of a temperature target and lastly to quantify the trade-off between welfare losses and temperature overshoot on order-of-magnitude level of accuracy within the decision framework of a cost-effectiveness analysis (CEA) using the Model of Investment and Technological Development (MIND). In short, we determine subsidiary targets within our modelling framework that lead to equal losses or equal maximum temperature as the “parental” target.

By doing so, we exploit the very working principle of CEA to derive the numerically closest counterpart of a temperature target one could achieve once a subsidiary target metric has been decided upon. As these numerical values are constructed solely by internal dynamics of the system, we call them “internal targets”. We also compare them to prominent subsidiary target values as given in the literature such as “1000 GtC” for the emission budget (Meinshausen et al., 2009).

Four types of subsidiary targets are investigated: all-time cumulative emissions, time-limited cumulative emissions (Meinshausen et al., 2009; Allen et al., 2009), all-time concentration and time-limited concentration targets (den Elzen and van Vuuren (2007, Fig. 1, “Overshoot stabilization”) and Swart et al. (2002, Fig. 5)). Thereby, we first focus on the 2°C target and later generalize the results to other temperature targets.

5 This article is organized as follows. Section 2 introduces the model utilized and the welfare loss metric. It demonstrates the latter for the original 2°C target. Sections 3 and 4 solve the model for all-time and time-limited subsidiary targets, respectively. Section 5 compares the results to externally defined subsidiary target values from literature or policy. Section 6 concludes the findings of this article.

2 Methods: Decision-analytic framework, model, and loss metric

10 2.1 The decision making approach: cost-effectiveness analysis

In this work the decision-analytic framework cost-effectiveness analysis is applied. CEA currently represents a prominent decision-analytic paradigm in research of climate economics (IPCC WGIII, 2014, Chap. 6).

CEA does not consider damages caused by climate change over which tremendous uncertainty persists. It evaluates the most cost-efficient way to reach a predefined target. CEA can calculate the cost of different climate targets and policy makers choose
15 the preferred one or suggest additional targets to be researched. In practice, climate targets have proven to be negotiable and reached a consensus at the Conference of the Parties 21 in Paris where the 2°C target was once again approved (COP21, 2015, “Paris Agreement”).

We follow the standards of (IPCC WGIII, 2014, Chap. 6) and apply CEA here in terms of its deterministic version that would not explicitly consider uncertainty in the climate system. As shown in Held et al. (2009) and Neubersch et al. (2014)
20 such a simplified approach has a fair chance of allowing for approximate scenarios, compared to those that would have been obtained from explicitly taking uncertainty into account for decision-making.

2.2 Model of Investment and Technological Development (MIND)

The Model of Investment and Technological Development is used to evaluate the formulated research questions. MIND is an IAM and was first developed by Edenhofer et al. (2005). Neubersch (2014) further extended the model to its latest development
25 stage that includes the new decision theoretic approach cost-risk analysis and up to date data. A simplified, deterministic CEA version of Neubersch (2014) is used in this work. Other development steps of MIND are for example Held et al. (2009), in which uncertainty was introduced and Lorenz et al. (2012) which added the possibility of learning.

MIND implements CEA in the modeling language General Algebraic Modeling System (GAMS) and solves the inter-temporal optimization problem using the CONOPT (<http://www.conopt.com/>) solver. It optimizes the period from 2015 to
30 2200 in time steps of five years. This time period is reasonable and sufficient for most applications because until 2200 even the unconstrained business as usual (BAU) scenario transitions into renewable energy sources (Edenhofer et al., 2005).

Calibration data for the fossil sectors reaches back to 1965. The population path is exogenous and assumes a growth until 2100 to 9.5 billion people where it stabilizes (Van Vuuren et al., 2003).

MIND takes the perspective of a global social planner. No regions are resolved and it is assumed that all policies are
35 implemented perfectly.

The model consists of three modules, see Fig. 1: A Ramsey-type growth model (growth module) which contains budget and production equations, the energy system (energy module) that resolves different energy production technologies and finally a

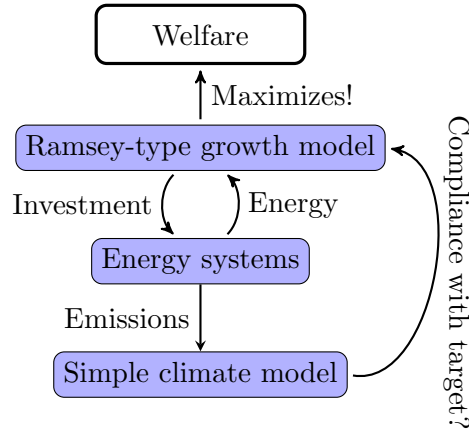


Figure 1. Stylized structure of CEA in MIND.

simple, energy-balance type climate model (climate module). The overall target is to maximize welfare under compliance with the target. Investments are made into different energy systems which produce energy and emissions. Energy feeds back into the growth module as a production factor while the emissions are fed into the climate module to assess compliance with the climate target. Here only the climate module is explained in detail, as it is important for our considerations. The other modules are explained in detail in Edenhofer et al. (2005), Roth et al. (2015) and Neubersch (2014).

2.2.1 Climate module

The numerical optimization process in GAMS requires too many iterations to apply a full-fledged Earth System Model (ESM) during the optimization and there is a need for simple climate models reproducing the stylized features of climate change. Accordingly MIND utilizes a simple climate model as well.

MIND’s climate module is based on the linear impulse-response model of Hasselmann et al. (1997). In its differential form, which is used here, it was introduced by Petschel-Held et al. (1999) and explained further by Krieglner and Bruckner (2004). To our understanding the underlying idea interprets the Holocene climate state as an equilibrium from which anthropogenic forcing would cause “small” excursions. The model of Petschel-Held et al. (1999) simulates the global mean temperature response to anthropogenic greenhouse gas (GHG) emissions in the following three equations.

The model reads as follows:

$$\dot{F} = E \tag{1}$$

$$\dot{C} = \beta E + BF - \sigma C \tag{2}$$

$$\dot{T} = \mu (\ln(c) + f_{SO_2} + f_{OGHG}) - \alpha T \text{ with } c = \frac{C + C_{pi}}{C_{pi}} \tag{3}$$

where the following variables and parameters are being used:

- E Anthropogenic CO₂ emissions
- F Cumulative anthropogenic CO₂ emissions
- C_{pi} Pre-industrial atmospheric CO₂ concentration
- C Atmospheric CO₂ anomaly w.r.t. to C_{pi}
- T Global mean temperature anomaly with respect to preindustrial climate

- f_{OGHG} radiative forcing from other greenhouse gases (OGHG)
- f_{SO_2} radiative cooling from SO_2 , a combustion by-product in coal power plants
- β Emission to concentration change rate conversion
- B Ocean and Biosphere carbon source
- 5 – σ Ocean and Biosphere carbon sink
- α Climate response rate
- μ Radiative forcing normalized by effective ocean heat capacity.

The quasi-linear model simulates the first order deviation from the pre-industrial climate. The total radiative forcing consists of CO_2 , SO_2 forcings and forcings by OGHG.

10 A shortcoming of the model is an overestimation of “the carbon dioxide uptake in the long run by neglecting the comparatively long time scales of the deep ocean as well as nonlinear effects like the decreasing solubility of CO_2 in seawater” (Kriegler and Bruckner, 2004).

In the following we utilize the parameter settings from (Kriegler and Bruckner, 2004), validated therein for the mappings “emissions on concentration” as well as “emissions on temperature”. The parameters are as follows, referring to a pre-industrial
15 temperature of 14.6°C .

- $C_{\text{pi}} = (280 \text{ ppmv})$
- $\beta = 0.47 \text{ ppmv GtC}^{-1}$
- $B = 0.00151 \text{ ppmv (GtC a)}^{-1}$
- $\sigma = 0.0215 \text{ a}^{-1}$
- 20 – $\alpha = 0.0447 \text{ a}^{-1}$
- $\mu = 0.1807 \text{ }^\circ\text{C a}^{-1}$

From the calibration of α and μ we conclude an equilibrium climate sensitivity of 2.8°C (Kriegler and Bruckner, 2004) and a transient climate response of 1.9°C (Khabbazan and Held, 2017, Eqn. 3). In Khabbazan and Held (2017) it was found that the 1-box model as described above excellently emulates the forcing-to-temperature mapping of GCMs. In fact, the average error
25 found is on the order of magnitude of the temperature standard deviation induced by natural variability. This could be achieved by choosing GCM- and scenario class-adjusted values for the box model’s equilibrium climate sensitivity and transient climate response, hereby deviating from the corresponding values as derived for the GCM. When utilizing correction formulas 9 and 10 in Khabbazan and Held (2017) the effective box model’s values would be 3.9°C and 1.9°C respectively. This means that the 1-box model excellently represents some GCM, regarding the temperature equation. For reasons of structural similarity we
30 expect the same to hold for the carbon cycle equation.

The sulfur emissions are directly coupled to the CO_2 emissions produced in the fossil energy sector. They have a cooling effect but only a lifetime of weeks to months, which is small compared to the lifetime of CO_2 (IPCC WGI, 2013). The exogenous path for OGHG is taken from the most ambitious representative concentration pathway (RCP), namely from the RPC2.6 which is described in Meinshausen et al. (2011b).

2.3 Metrics of comparison

2.3.1 Mitigation cost metric: Balanced Growth Equivalent

In this work, mitigation cost are measured in reduction of Balanced Growth Equivalent (ΔBGE) (Anthoff and Tol, 2009). Following the interpretation of Anthoff and Tol (2009) and Mirrlees and Stern (1972) $\Delta BGE_{X,Y}$ denotes a relative consumption difference between scenario X and Y. $\Delta BGE_{X,Y} = 1\%$ means that in scenario Y the consumption in each time step is 1% lower than in scenario X. Hereby the consumption loss is not measured for the original scenarios X and Y, but for stylized scenarios X' and Y' derived from linearly scaling an exponentially growing consumption scenario such that the welfare level of X' matches that of X, and the welfare level of Y' matches that of Y.

In this work, we compare different climate policy scenarios X against the 2°C scenario. We are interested whether X is cheaper or more expensive than the 2°C scenario in units of the 2°C scenario cost. Hence, we normalize $\Delta BGE_{BAU,X}$ by dividing by $\Delta BGE_{BAU,2^\circ C}$. Hereby “BAU” denotes “business as usual”, the former reference case denoting no climate policy active. In this article we strive at demonstrating an analytic principle by utilizing the simplest-possible climate module for the sake of transparency. In this vein we can also approximate a “baseline case” IPCC WGIII (2014, Glossary) that would include already announced policy measures by BAU. The difference is rather small compared to the policy / no policy intercomparison.

2.3.2 Climate metrics: maximum temperature

Schneider and Mastrandrea (2005) discuss two metrics for climate risk: maximum temperature and – as introduced by them – the degree years by which a temperature profile transgresses a certain target.

The maximum temperature is simply defined as $T_{\max} = \max_t T(t)$, t being the time. The Paris Agreement of COP21 (2015) and WGBU (2004) formalized their targets in this metric. The advantage of this metric is the clear indication of the peak warming. The drawback is its ignorance of the duration for which high temperatures persist. In contrast, the metric of degree years (Schneider and Mastrandrea, 2005) measures the persistence of high temperatures but does not indicate peak heights.

2.4 Demonstration of the model with the all-time 2°C target

The following sub-section describes the reference scenario of our analysis: the cost-effective 2°C scenario. Hereby we note that (COP21, 2015) does not mention a termination year for this upper limit. We interpret this as an upper limit that is active virtually up to infinity. While this is exactly the scenario as already calculated by Edenhofer et al. (2005) here actualized prescriptions in terms of historic emission trajectories are utilized. Hence the reader is enabled to compare like with like, when cost-effectiveness analyses of alternative targets are presented thereafter.

Fig. 2 shows the different climate variables in the BAU and $T(\forall_t) \leq 2^\circ C$ scenarios. Fig. 2(a) displays the temperature time series of the simulations. The temperature in the all-time 2°C scenario reaches 2°C in 2060 and remains there till the end of the simulation. The temperature in the BAU scenario peaks at 4.43°C in 2160 and then starts to decline slightly, due to the sudden decline in emissions, cf. Fig. 2(b).

Fig. 2(b) shows the emission time series of both scenarios: In the BAU scenario, emissions increase until about 2110 and then decrease sharply to approach values close to zero towards the simulation end. This sudden decrease is caused by scarcity effects for fossil fuels, which become strong enough until 2110 such that renewable energy production takes over without any climate policy (Edenhofer et al., 2005). The emission profile of the 2°C scenario in Fig. 2(b) starts to decrease promptly when the simulation is started, indicating that a 2°C climate policy requires immediate and sudden actions because delaying

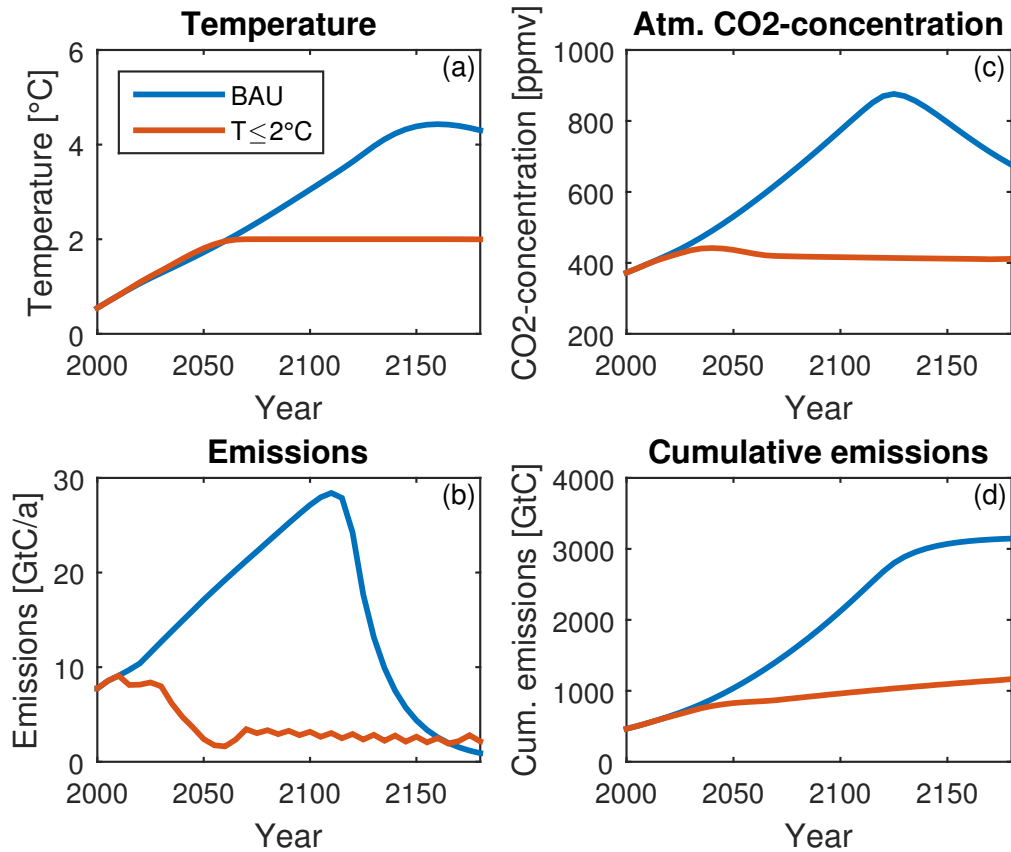


Figure 2. MIND results for the BAU and 2°C scenario. The balanced growth equivalent loss is $\Delta BGE_{2^\circ\text{C},\text{BAU}} = 0.77\%$. The plots are showing (a) temperature, (b) atm. CO₂ concentration, (c) yearly emissions and (d) cumulative emissions.

mitigation causes a significant increase of mitigation costs. This has been reported for the MIND model by Roth et al. (2015) and more general already by Nordhaus (1994).¹

Fig. 2(c) shows the atmospheric CO₂ concentration in ppmv. The numbers displayed here are not CO₂eq concentrations, but pure CO₂. The design of MIND solely calculates CO₂ endogenously, whereas other greenhouse gases (OGHG) such as N₂O and CH₄ are prescribed exogenously (Neubersch, 2014). Concentrations expressed in ppmvCO₂ represent pure CO₂ concentrations, while ppmvCO₂eq measures CO₂ equivalents (See Appendix C for more information). The BAU scenario reaches very high concentrations and peaks in 2125 at ≈ 850 ppmv. The concentration time series of the 2°C scenario peaks at 441.8 ppmv in 2040 and drops slightly till 2070 to values between 410 and 420 ppmv. The slight decrease is caused by the effect that decreasing emissions lead to decreasing cooling by SO₂ agents and hence lower pure CO₂ concentrations are allowed for the same temperature.

Fig. 2(d) shows the cumulative emissions time series for the BAU and 2°C scenarios. The data in the graph is the integral over Fig. 2(b). The behavior is similar to the other climate variables: BAU rises fast until 2125 and then levels off as emissions in Fig. 2(b) fall to zero.

¹The wiggles observed in the 2°C emission profile show a numerical artifact, the optimum of this period is so flat that the numerical optimizer reaches its termination criteria before smoothening them out. This is a known problem and ongoing research is improving the optimization routines.

From 2040 onwards the 2°C scenario significantly deviates from the BAU scenario cumulative emissions. Between 2040 and the end of the simulation period the increase is nearly linear². If the simulation would run over a longer time period, cumulative emissions would further increase until renewables become cheap enough to out-compete fossils. The concentration equation Eq. (2) explains why for a constant temperature, increasing cumulative emissions are possible. Assume $C_{2^\circ\text{C}}$ to be the concentration that leads to 2°C in the steady state of the temperature equation Eq. (3). The steady state of the concentration equation then gives

$$E = \frac{1}{\beta} (BF - \sigma C_{2^\circ\text{C}}). \quad (4)$$

Hence, in our climate model emissions only need to cease totally for $BF = \sigma C_{2^\circ\text{C}}$. This means if cumulative emissions reach

$$F_{2^\circ\text{C}} = \frac{\sigma}{B} C_{2^\circ\text{C}} \approx 6538 \text{ GtC} \quad (5)$$

emissions have to come to absolute zero. This value is more than twice of the cumulative emissions at the simulation end of the BAU scenario, which are 3158 GtC. As the BAU scenario already ceases emissions without climate policy, only by scarcity of fossils and learning effects of renewables, the energy system does not reach this limit under a mitigation target either. However, the simulation of the 2°C scenario accumulates 1216.7 GtC of emissions by 2200, therefore cumulative emissions would continue to rise in the 2°C scenario if the simulation period was extended. Nevertheless, for the energy transition, this and the next century are of importance. Therefore, our considerations and simulations of cumulative emissions only reach until 2200 and we interpret $F(t = 2200)$ as the all-time cumulative emissions.

Table 1 shows the relevant metrics of comparison for the simulations in Fig. 2.

3 All-time targets

First we search for all-time cumulative emissions and concentrations targets within our model that do not exceed 2°C or that cause the same mitigation cost as the all-time 2°C target. This is done by sampling over many possible all-time concentration and cumulative emissions targets. The concentration sampling range is $C(\forall_t) \in (400, 1000)$ ppmv. The lower boundary is given by today's CO₂ concentration and the upper by the concentration peak of the BAU scenario in Fig. 2. The cumulative emissions sampling range spans $F(\forall_t) \in (600, 3200)$ GtC. The lower value is chosen to be close to the lowest feasible target, which is at $F(\forall_t) \leq 640 \pm 5$ GtC. The upper margin is given by the all-time cumulative emissions of BAU. So all possible targets are covered.

3.1 All-time targets that peak at 2°C

Fig. 3 shows the result of the sampling and the identified all-time cumulative emissions and concentration targets that peak at 2°C warming. In both framings, the subsidiary targets that comply with peak warming of 2°C lie close to the feasibility limit. The curves displayed in this figure are derived from internal properties of the system under investigation. Hence we call the numerically determined 2°C-equivalent subsidiary targets, “internal targets” (as against “external targets” set by a political process – see section 6). In our model, they represent the closest-possible substitutes of the 2°C target.

The time series of the climate variables of the identified subsidiary targets are shown in Fig. 4. Both subsidiary targets peak at 2°C. The cumulative emissions target peaks early, around 2060, jointly with the 2°C scenario but then falls to 1.4°C in 2180, unlike the concentration target which asymptotically approaches 2°C. In all mitigation scenarios emissions drop in Fig. 4

²The wiggles of Fig. 2b are not visible anymore as the integration smoothens them.

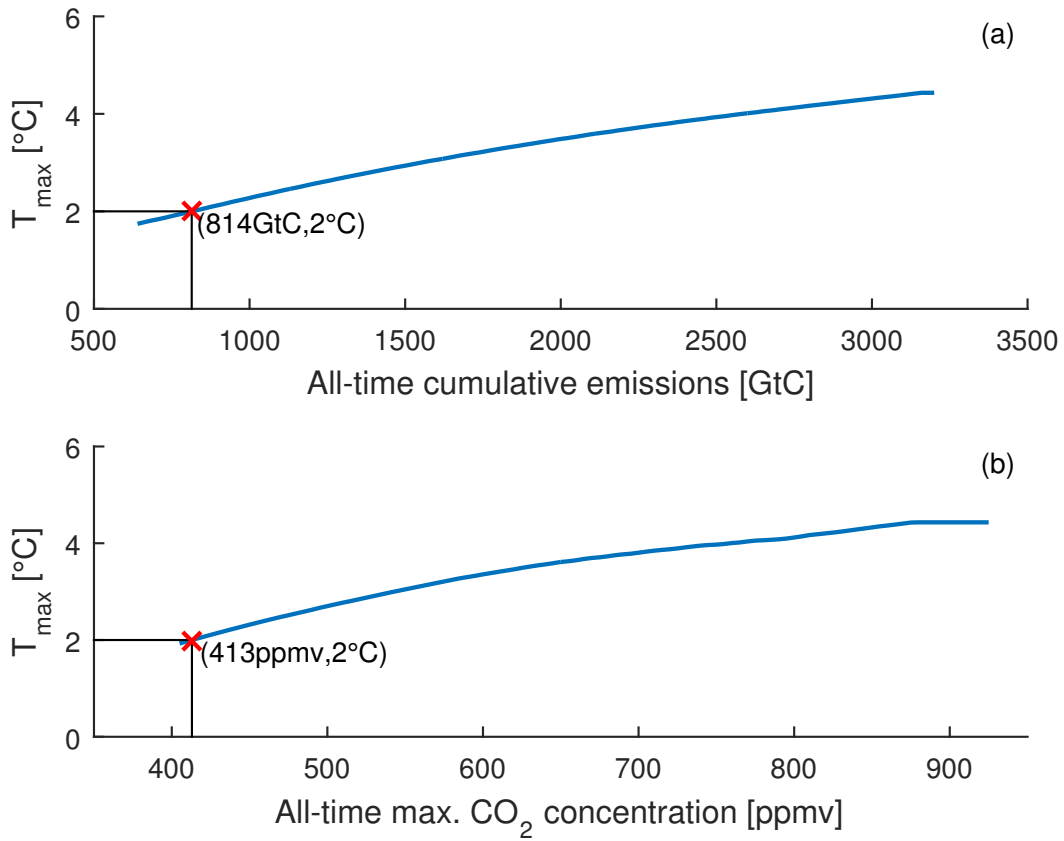


Figure 3. Sampling over the feasible span of cumulative emissions (a) and concentration (b) targets. A red “x” marks the target values that hit 2°C.

(b) and (d). For the concentration target the drop occurs the earliest but does not reach zero. Eq. (5) showed that requiring a constant concentration allows for more cumulative emissions than the BAU scenario. Hence, under a concentration guardrail emissions do not reach zero.

Further, the theoretical stable concentration for 2°C can be calculated using Eq. (3). For an unchanging temperature we set $\dot{T} = 0$ and get:

$$C = C_{\text{pi}} \cdot \exp\left(\frac{\alpha}{\mu} T - (f_{\text{SO}_2} + f_{\text{OGHG}})\right). \quad (6)$$

If the SO₂ and OGHG forcing were absent we could derive a radiative forcing purely driven by CO₂ which resulted in a stable concentration for 2°C of 459 ppmvCO₂.

This is higher than the numerically determined value of 413 ppmvCO₂ because SO₂ and OGHG are neglected for the theoretical value. Hence, the OGHG forcing outweighs the SO₂ cooling. (The exponential function is strictly monotonic and $f_{\text{SO}_2} \leq 0$ and $f_{\text{OGHG}} \geq 0$. To obtain a lower concentration value in Eq. (6) the sum of $f_{\text{SO}_2} + f_{\text{OGHG}} > 0$ and hence $|f_{\text{SO}_2}| < |f_{\text{OGHG}}|$.)

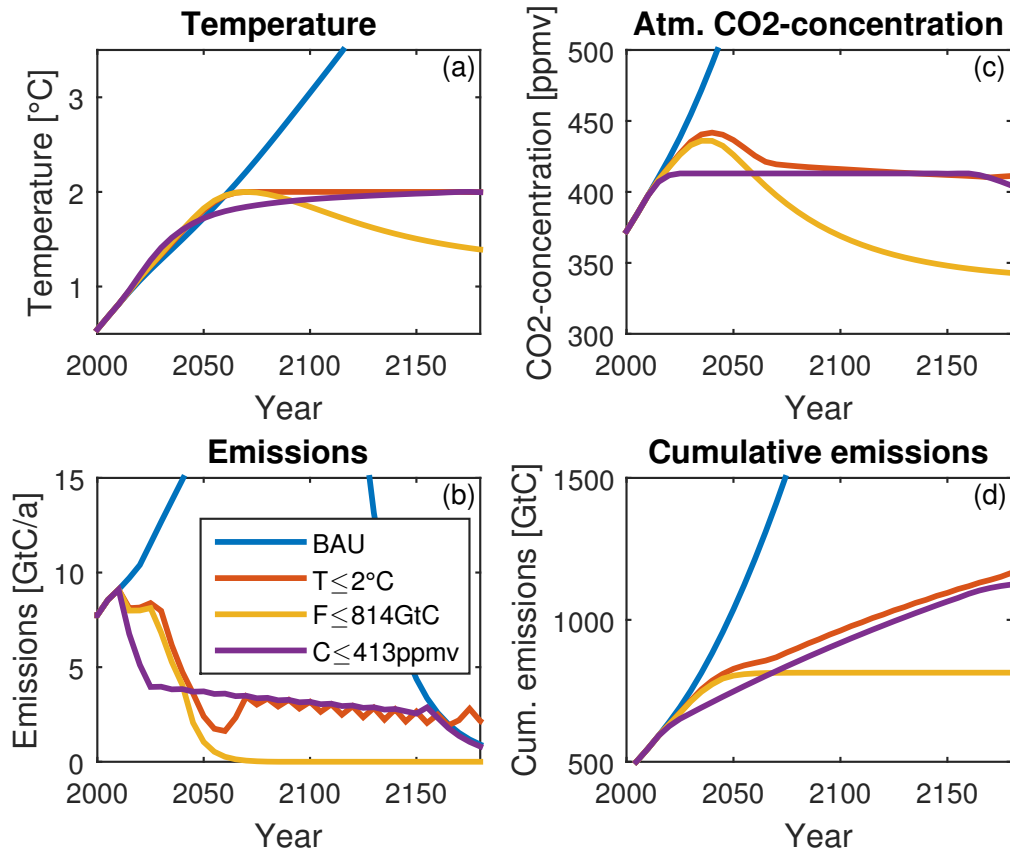


Figure 4. Temperature (a), emissions (b), concentration (c) and cumulative emissions (d) for BAU, all-time 2°C , $F(\forall_t) \leq 814 \text{ GtC}$ and $C(\forall_t) \leq 413.0 \text{ ppmv}$.

3.1.1 CO_2 and CO_2eq concentrations.

The identified subsidiary concentration target is expressed in pure CO_2 concentrations. Along this target, we like to show the difference between pure CO_2 and CO_2eq concentrations. Both the pure CO_2 and CO_2eq concentrations are plotted in Fig. 5 using the method of Appendix C. CO_2eq concentration (blue) reaches its maximum in 2020 at 497 ppmvCO_2eq clearly above the pure CO_2 concentration of 413 ppmvCO_2 (red) and the theoretical steady state CO_2eq concentration for 2°C of 459 ppmvCO_2eq .

3.1.2 Economic losses of the all-time targets that peak at 2°C .

The results in Tab. 1 show that the cumulative emissions target causes 20% higher losses and the concentration target 50% higher losses than the sole 2°C target. This cost difference is caused by the early emissions reductions that are realized in the concentration subsidiary target. The earlier and the stronger the mitigation is applied the costlier it is. Even though the cumulative emissions target drops to zero emissions around 2065 and the concentration target remains around 3.5 GtC/yr , the concentration target is more expensive. Hence, the early mitigation causes the major part of the losses. This can also be seen in the concentration time-series of Fig. 4(c), where the concentration of the cumulative emissions (yellow) follows the concentration of the 2°C scenario (red) to levels above the concentration guardrail of 413 ppmv .

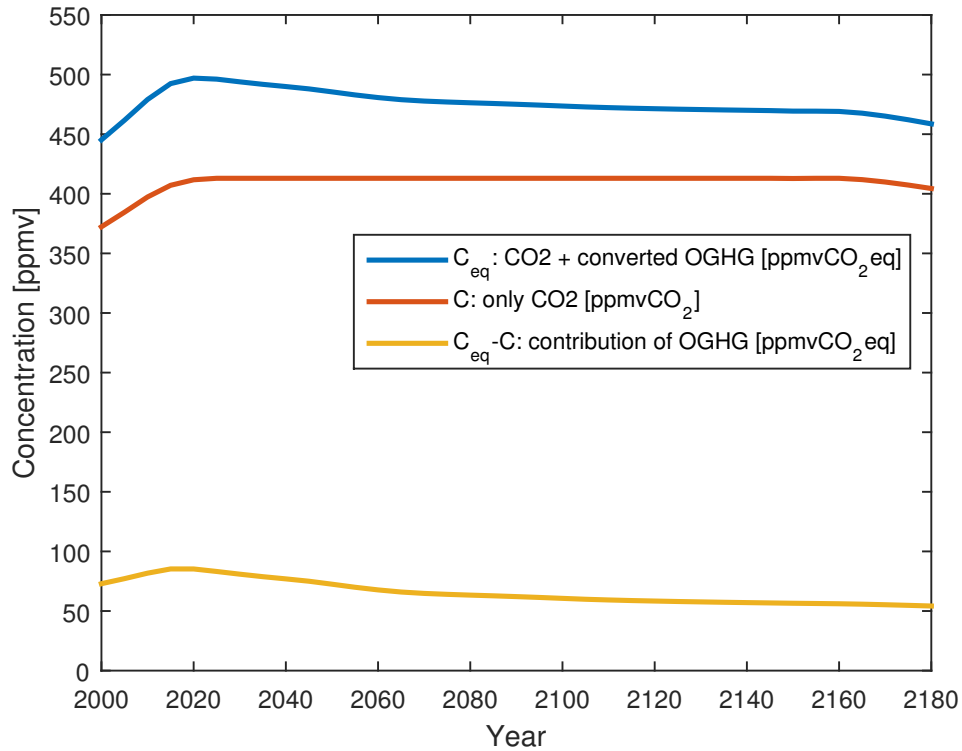


Figure 5. CO₂ and CO₂eq concentrations for $C(\forall_t) \stackrel{!}{\leq} 413.0$ ppmvCO₂.

Our result shows: If a subsidiary all-time target is designed not to transgress 2°C, the cumulative emissions framing is preferable over the concentration framing. The loss increase from 2°C to the cumulative emissions target is caused by the strong continued mitigation (emissions drop to zero) which lead to decreasing temperatures after 2060 in the cumulative emissions scenario. The 2°C scenario remains at 2°C. It is up to debate whether the 20% cost increase is bearable in exchange for the reduced degree years.

The cost difference between the cumulative emission and the concentration subsidiary targets stems from the timing of the emission decrease. In the concentration framing, emissions have to decrease 20 years earlier than in the cumulative emission scenario, see Fig. 4(b). It can be seen best in the concentration time-series (Fig. 4(c)) of the different framings. The 2°C and the subsidiary cumulative emission targets are close to each other and both overshoot the concentration subsidiary target for some time. This allowance for an overshoot causes lower losses.

3.2 Generalization of the result for different temperatures and costs

Fig. 6 displays the relation between normalized BGE losses and the maximum temperature within three different all-time framings: temperature ($T(\forall_t) \leq T_{max}$), concentration ($C(\forall_t) \leq C_{max}$) and cumulative emissions ($F(\forall_t) \leq F_{max}$). The previously found result is confirmed over the full range of possible maximum temperatures. The losses of the C targets are above the losses of the F targets. This means, whatever temperature a climate policy aims to achieve, it is best for the economy to follow the investment path provided by an IAM that is explicitly constrained with the temperature aim. If this is impossible, a cumulative emission target should be preferred over a concentration target.

Further, within the range from 2 to 3.5°C, the distance between the red and the yellow curve increases. Hence, for higher temperatures, the choice of the framing has a more severe impact on the losses.

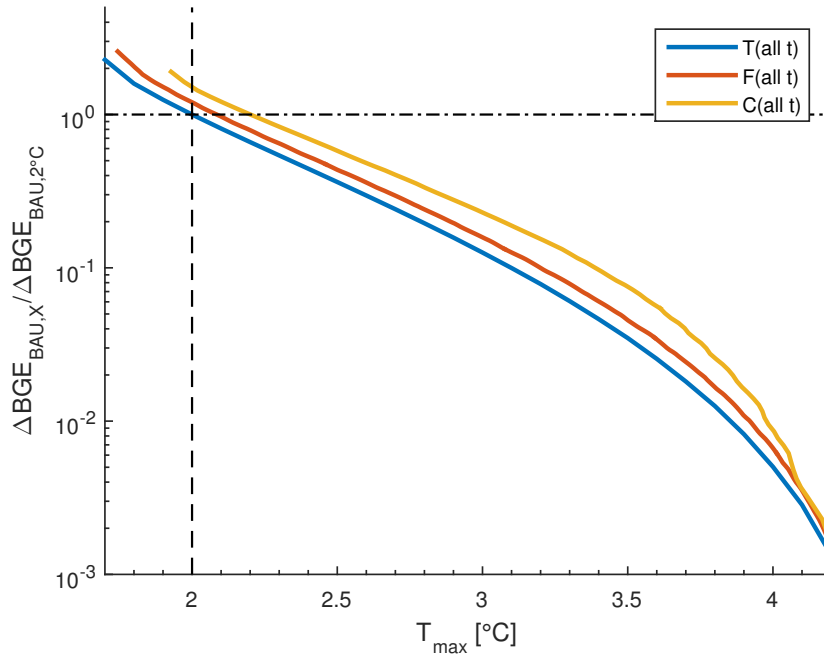


Figure 6. BGE losses (log scale) versus maximum temperature for three all-time climate target framings. Concentration and cumulative emissions data is based on the sampling of Fig. 3. Temperature data is based on new sampling over $T(\forall t) \leq T_{\max} \in (1.7, 4.2)^\circ\text{C}$. The differently dashed lines illustrate the relation to Fig. 7.

Fig. 7 shows this nexus from a different perspective. The differently dashed lines connect Fig. 6 and 7. Plot 7(a) displays the relative increases in losses if a pure temperature target is substituted by a cumulative emissions (yellow) or concentration target (red). For cumulative emissions targets the relative increase of losses from its corresponding temperature target varies within a range of 20 to 40%. In the temperature range from 2–3°C it is confined within 20–30%. The concentration targets cost between 50 and 120% more than their equivalent temperature target in the range of 2–4°C. For temperatures above 4°C the curves converge again, as they get close to the BAU scenario.

Fig. 7(b) plots the temperature overshoot of different framings if only a certain loss is allowed. Depending on the target framing a fixed loss leads to different maximum temperatures. Again the cumulative emissions vary within a more confined range ($\leq 0.1^\circ\text{C}$) than the concentration targets ($\leq 0.3^\circ\text{C}$). Also as in (a), for scenarios similar to BAU, the targets approach each other again (i.e. for losses $\rightarrow 0$). For concentration targets, the highest overshoot of 0.3°C is observed for losses of $0.1 \times \Delta BGE_{\text{BAU},2^\circ\text{C}}$, which corresponds to $T_{\max} = 3^\circ\text{C}$.

In conclusion, losses increase by 20–120% if temperature targets are expressed in a different all-time framing. If, on the other hand, losses are set equal, peak warming results up to 0.3°C higher. Over the full temperature range that our model allows, all-time cumulative emissions targets should be preferred over all-time concentration targets.

4 Time-limited targets

The following sections investigate time-limited targets, elaborate their features and compare them against all-time targets.

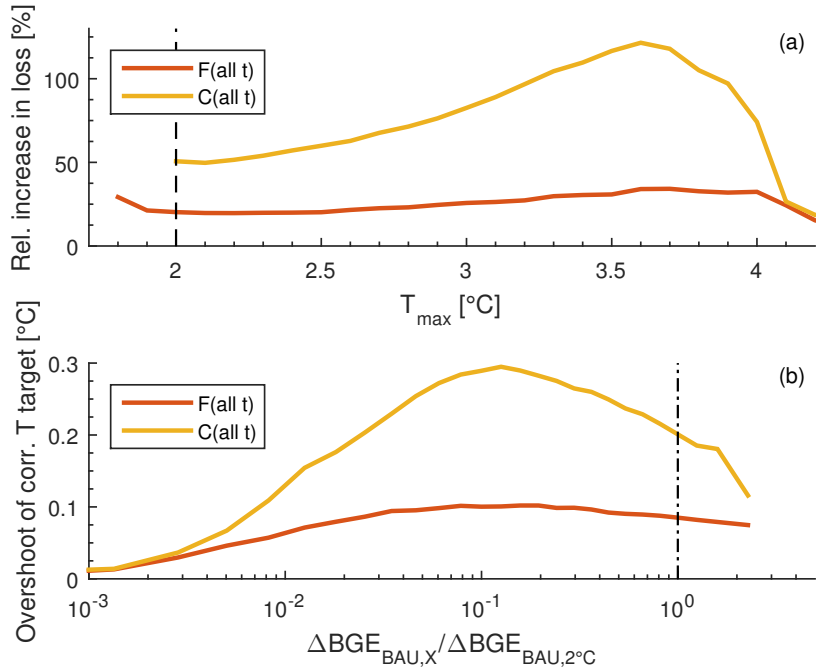


Figure 7. Relative increase in losses (a) over the maximum temperature if a temperature target is substituted by a cumulative emissions (red) or concentration target (yellow). Temperature overshoot (b) over normalized losses.

4.1 Time-limited concentration targets

Time-limited concentration targets allow a concentration peak before declining to a stable level. This pattern is shown by the concentration time series of the 2°C target in Fig. 2(c). As temperature lags behind the concentration, a concentration overshoot can be used to attain a stable temperature earlier than in the corresponding all-time target. In Appendix D we analytically argue why this is the case.

4.1.1 A 2°C compatible time-limited concentration target.

Moreover, allowing an initial overshoot is economically beneficial, as it is the early mitigation that is most costly.

Fig. 8 shows the maximum temperatures (contours and color) of concentration targets (ordinate) that have been applied from different years (abscissa) onwards. The white space depicts the infeasible region. Staying below 2°C is close to the infeasibility border. However, there are many combinations of application times and concentration values that lead to a maximum warming of 2°C. Point **A** and **B** mark two possible combinations, serving as reference points in the following discussion. **A** is chosen as the last point of the stable region, where maximum temperature does not change with application time. Its coordinates are (2060, 413 ppmv). The application time 2060 years coincides with the time where concentration in the 2°C scenario stops its fast decay; the concentration value is equivalent to the all-time concentration target that hits 2°C, *cf.* Fig. 4. Point **B** (2160, 346 ppmv) is arbitrarily chosen within the regime where concentration values decrease with application year.

4.1.2 Two time-limited concentration that stay below 2°C.

Fig. 9 shows the time-limited concentration targets **A** and **B**. Plot (a) shows that both targets do not transgress 2°C.

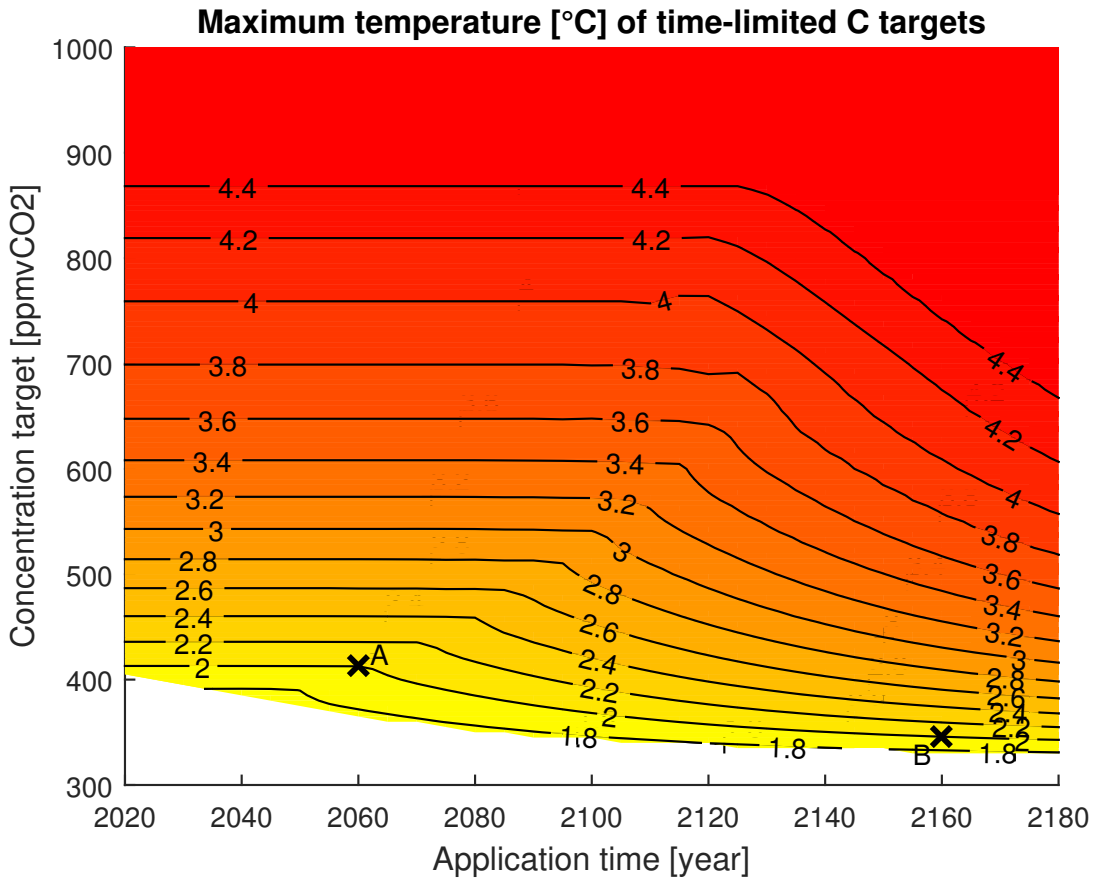


Figure 8. Maximum temperatures (color and contours) for concentration targets that are applied from different years onwards; **A** and **B** are exemplary targets staying below 2°C.

Scenario **A** (yellow) stays close to the 2°C scenario over the full simulation time. The concentration time-series of **A** has the characteristics of a concentration overshoot followed by a stable plateau. Its losses are 12% higher than in the pure 2°C target and hence lower than the all-time cumulative emissions target (20%) of the previous section.

Scenario **B** (purple) is nearly equivalent to the all-time cumulative emissions target of the previous section, *cf.* Fig. 4. Temperature peaks early in 2060 and declines to 1.4°C in 2180, likewise the all-time cumulative emissions target. The final cumulative emission value is 810 GtC slightly smaller than the cumulative emissions target. This is in accordance with the higher loss of 22%, 2% more than the cumulative emissions scenario. The results are summarized in Tab. 1.

4.1.3 Losses of time-limited concentration targets.

Fig. 10 displays the normalized BGE losses in units of $\Delta BGE_{BAU,2^\circ C}$. Points **A** and **B** lie on the 2°C contour line (dashed). The structure of the losses is similar to the structure of the maximum temperatures of Fig. 8. However, the losses begin to decline earlier with increasing application time than maximum temperatures decrease. Hence, **A** has the lowest possible losses while staying below 2°C and is therefore a good choice. The white region at the lower end of the graph again illustrates the infeasible region. The infeasibility does not originate from economic factors but from the climate system. No carbon dioxide removal is implemented and hence the limiting factor is the natural carbon uptake of the climate model. The maximum losses possible are

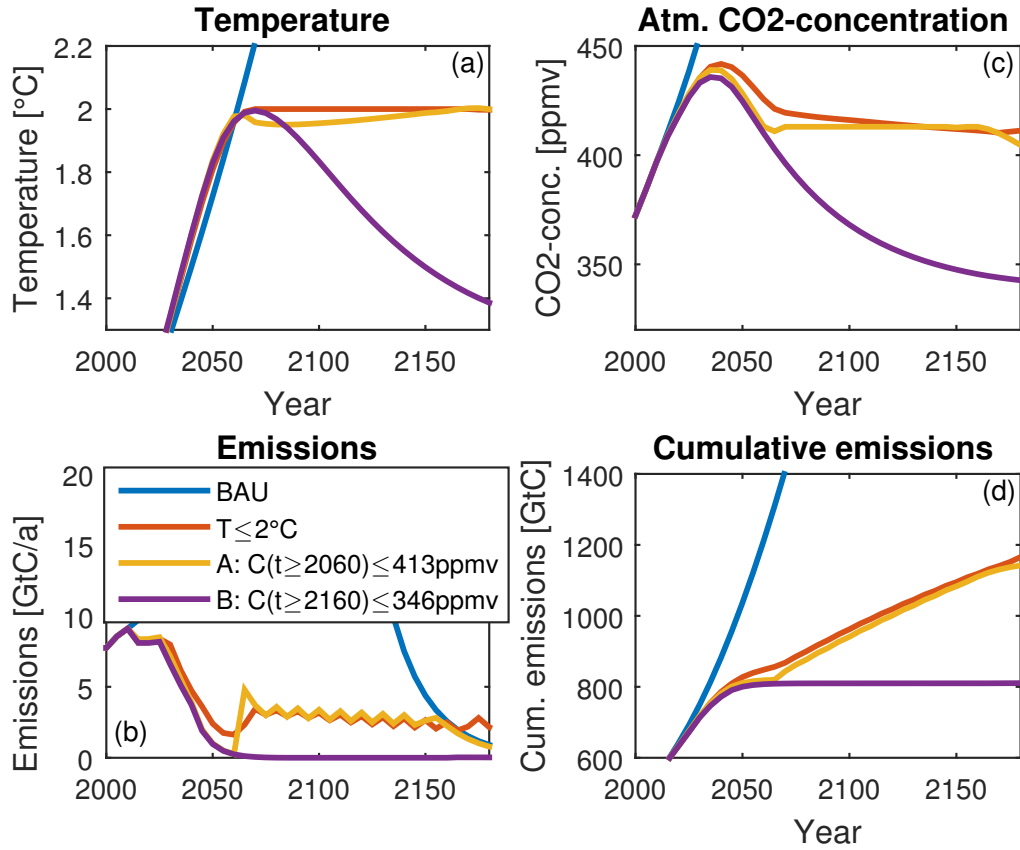


Figure 9. Climate variables of the scenarios: BAU, all-time 2°C, **A**: $C(t \geq 2060) \leq 413$ ppmv and **B**: $C(t \geq 2160) \leq 346$ ppmv.

4.2 Time-limited cumulative emissions targets

Concerning time-limited cumulative emissions targets, we restrict ourselves to targets that integrate emissions only up to a point t_e in the future. This can be interpreted as a policy that is running only until a certain point of time after which regulations are dropped again. We sample over $F(t \leq t_e) \leq t_e$ where $t_e \in (2020, 2200)$ and $F_{\text{target}} \in (500, 3200)$ GtC. The lower limit in F_{target} is given by the already emitted budget in 2015 and the upper limit by the maximum cumulative emissions the BAU scenario is reaching.

The earlier the cumulative emissions targets lose effectivity and the bigger the allowed budget, the higher is the resulting maximum temperature, see Fig. 11. The white space below the graph marks the feasibility limit. Cumulative emissions below 640 GtC are not feasible. This is identical to the all-time cumulative emissions target feasibility limit.

The targets that peak at 2°C are located on the lower right of Fig. 11. All targets peaking at 2°C lie below the isoloss line (bold dashed). With rising cumulative emissions, losses decrease. Hence, the targets peaking at 2°C of this framing are more expensive than pure the 2°C scenario.

The illustrative cases **C** and **D** are very similar to the all-time cumulative emissions target identified in Sec. 3 until they lose effectivity. Then they rise sharply in emissions.

Fig. 12 displays the losses of sampled time-limited cumulative emissions targets. Losses decrease with increasing emissions and earlier loss of effectivity. However, especially for low emissions budgets, losses are stable for a wide time span. Hence,

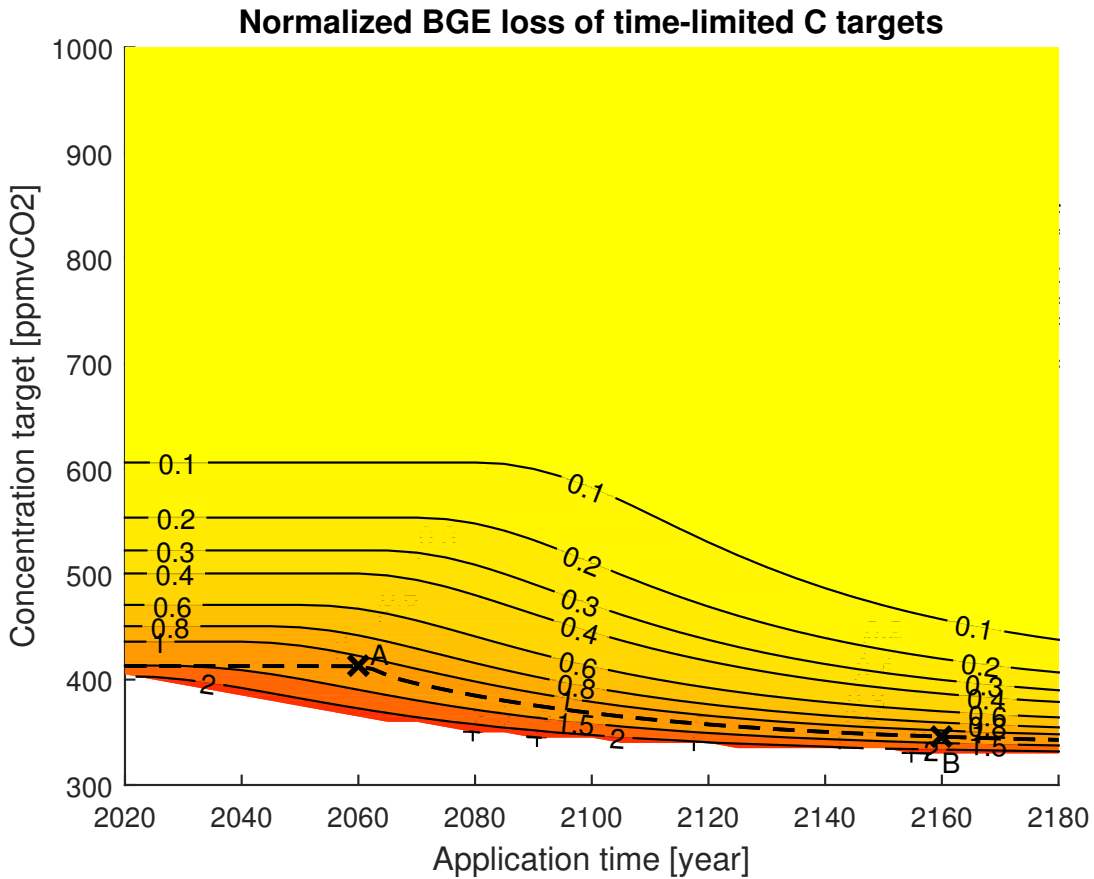


Figure 10. Normalized BGE loss in units of $\Delta BGE_{BAU,2^\circ C}$ (color and contours) for concentration targets that are applied from different years onwards; bold dashed line: the $2^\circ C$ peak warming contour from Fig.8.

whether for example $F(t \leq 2100) \stackrel{!}{\leq} 1000 \text{ GtC}$ or $F(t \leq 2150) \stackrel{!}{\leq} 1000 \text{ GtC}$ is applied has no influence on losses. Contrary to the peak warming (Fig. 11) which changes by nearly $1^\circ C$. This highlights again that it is the early mitigation, roughly in the 21th century, that determines the losses caused by mitigation policies.

5 External subsidiary target formulations

- 5 Besides targets that are internally consistent with our model, also external targets were investigated. Those external targets are not a priori comparable within the framework of MIND. Different climate models and integrated assessment models have been used when creating the above cited targets (IPCC WGIII, 2014). The following external targets are investigated:
 - limit cumulative emissions F for all time C emissions below one trillion tons as formulated by Allen et al. (2009):

$$\tilde{F}(\forall_t) \stackrel{!}{\leq} 1000 \text{ GtC}$$
 - 10 – stabilize atmospheric GHG concentration at 450 ppmvCO₂eq from 2100 onwards, which combines the stabilization demanded by United Nations (1992) with the concentration level formulated by IPCC WGIII (2014, Table SPM.1):

$$\tilde{C}(t \geq 2100) \stackrel{!}{\leq} 450 \text{ ppmvCO}_2\text{eq}$$

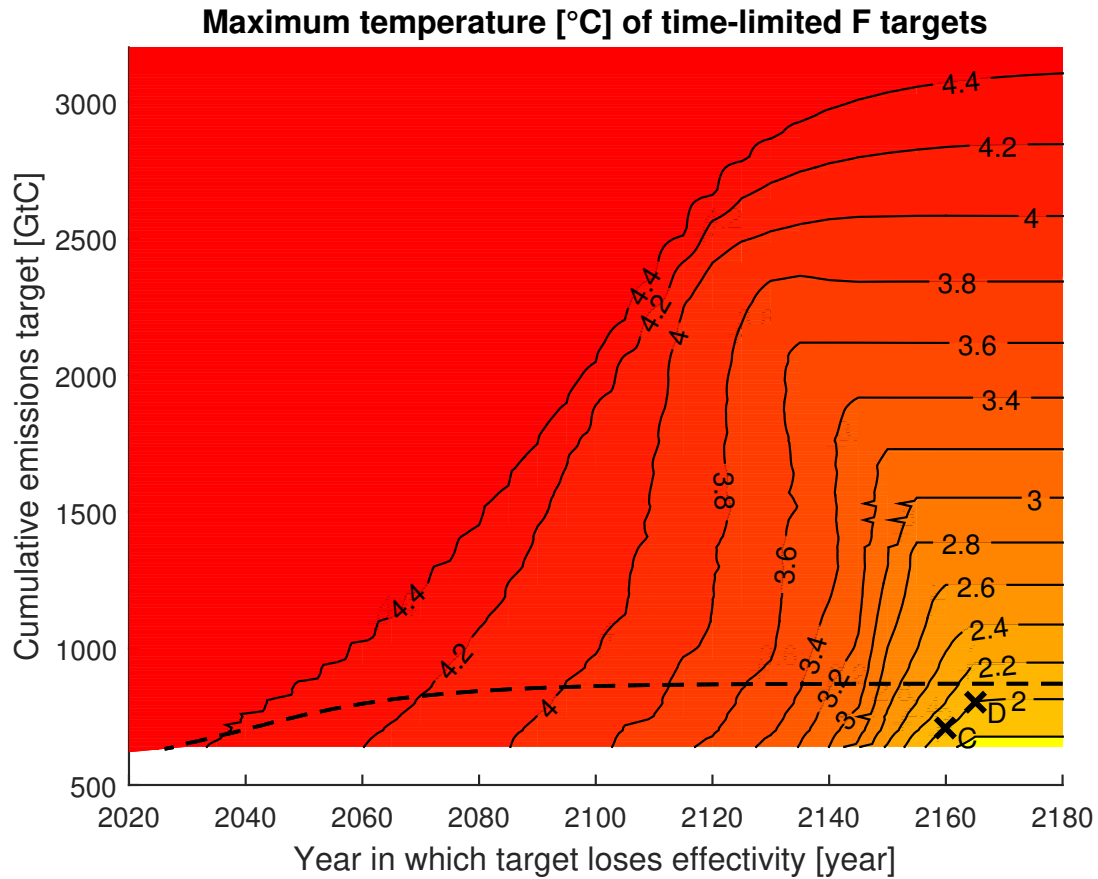


Figure 11. Maximum temperatures (color and contours) for cumulative emissions targets that lose effectivity from different years onwards; bold dashed line marks targets with losses of $1 \times \Delta BGE_{BAU,2^\circ C}$; two illustrative targets **C** and **D**.

5.1 The trillionth tonne.

The all-time cumulative emissions target of (Allen et al., 2009) exceeds $2^\circ C$ in our modeling framework. An equilibrium climate sensitivity (ECS) of $2.4^\circ C$ limits warming to $2^\circ C$ within our model under the constraint of maximum 1000 GtC of all-time cumulative emissions. By reiterating the studies concerning all-time cumulative emissions targets of Sec. 3 with ECS of $2.4^\circ C$ we find our results reaffirmed. Additional normalized losses still vary within 20 to 40% depending on the desired maximum temperature.

5.2 Stabilized concentration.

The stable concentration from 2100 onwards is expressed in CO_2eq . Hence, we force with a maximum CO_2eq concentration calculated according to Appendix C. OGHG add up to the equivalent concentration and the pure CO_2 concentration is therefore below 450 ppmv after 2100 as Fig. 13(c)(yellow) shows. However, before 2100 the pure CO_2 concentration peaks at 465 ppmv; CO_2eq concentration peaks at 550 ppmv. These peaks cause a maximum warming of $2.2^\circ C$ followed by declining temperatures (Fig. 13(a)). Between 2105 and 2110, temperature drops below $2^\circ C$ and stabilizes at $1.85^\circ C$. The losses caused by this target are $0.8 \times \Delta BGE_{BAU,2^\circ C}$ making it 20% cheaper than the pure $2^\circ C$ scenario. This decrease in losses is in exchange for temperature overshoot before 2100.

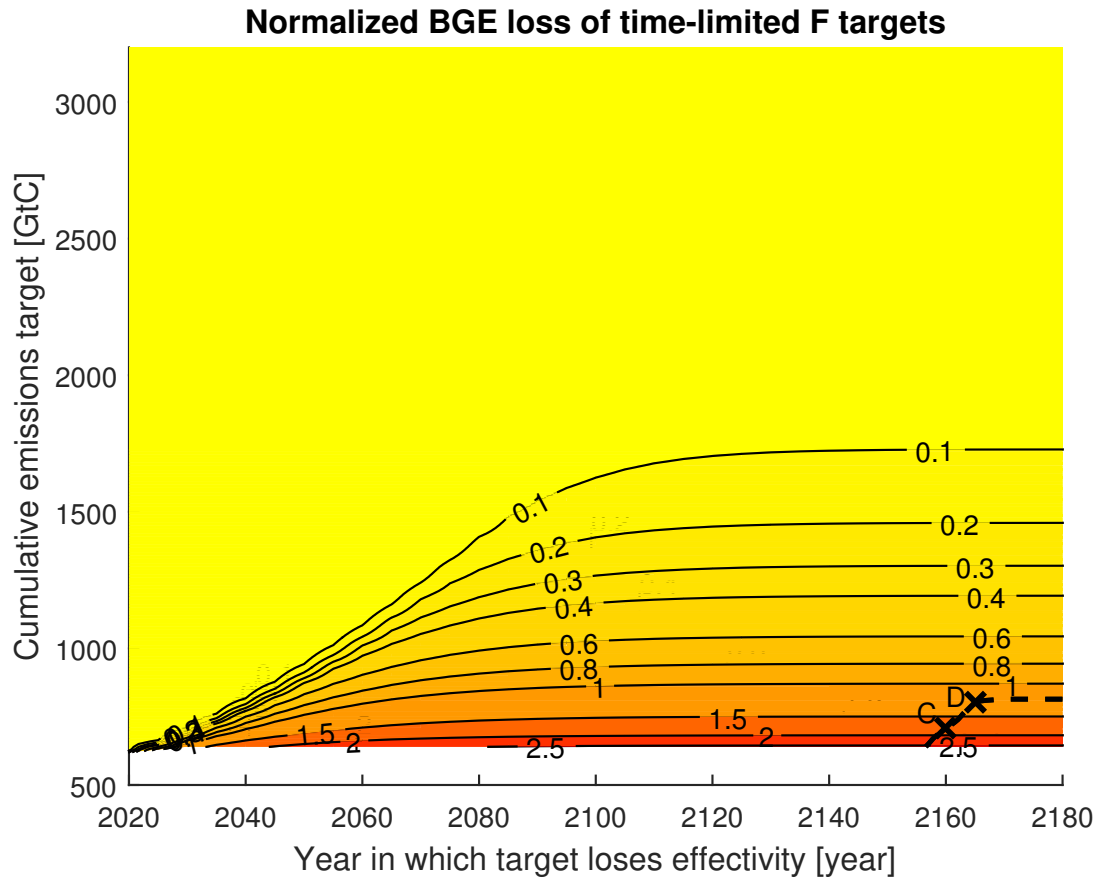


Figure 12. Normalized BGE loss in units of $\Delta BGE_{BAU,2^\circ C}$ (color and contours) cumulative emissions targets that lose effectivity from different years onwards; bold dashed line: the $2^\circ C$ peak warming contour from Fig.11.

If the concentration is only fixed in the year 2100 and then allowed to rise again, all variables jump up after 2100. Hence, a target that is only binding in 2100 is not a sensible target.

6 Conclusions

We introduced the concept of “internal targets” as closest-possible subsidiary versions of temperature targets. Within this concept we analyzed the trade-off between equal peak-warming and equal losses when different subsidiary climate targets are used. We investigated all-time temperature targets as well as all-time and time-limited atmospheric greenhouse gas concentration and cumulative carbon emissions targets. For the analysis we employed a deterministic Cost-Effectiveness-Analysis using the integrated assessment model MIND. The welfare maximizing model was forced with the mentioned guardrails and subsidiary targets with equal peak-warming and equal losses as the all-time $2^\circ C$ target were identified.

We found that losses increase by 20–120% if an all-time temperature target is expressed in a subsidiary all-time target. If losses are set equal, peak warming results up to $0.3^\circ C$ higher. Other possible trade-offs are found within this range.

Over the full evaluated temperature range ($\geq 1.8^\circ C$) all-time cumulative emissions targets cause lower additional losses (20% at $2^\circ C$ peak-warming) and lower temperature overshoot at equal losses ($0.1^\circ C$ at equal losses as the $2^\circ C$ scenario) than all-time concentration targets (50%, $0.2^\circ C$). See Table 1 for all results.

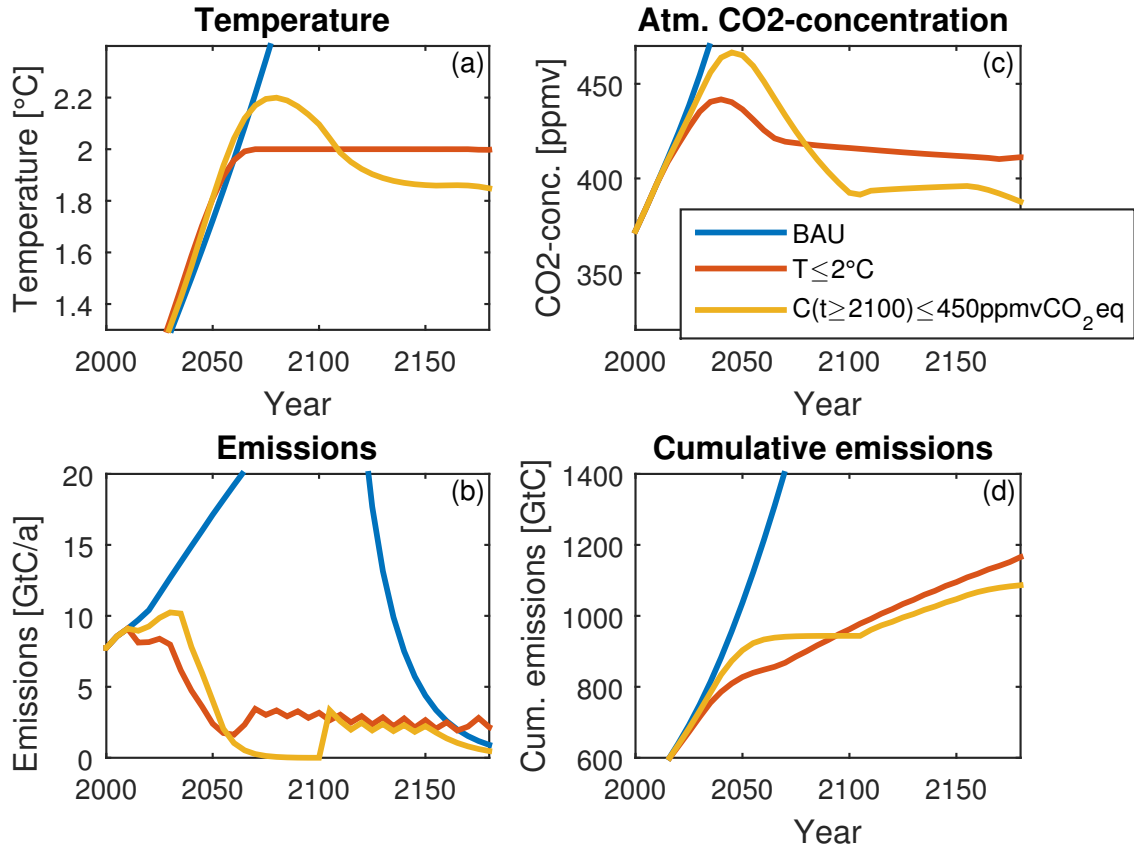


Figure 13. Climate variables of the scenarios: BAU, all-time 2°C and $C(t \geq 2100) \leq 450 \text{ ppmvCO}_2\text{eq}$.

Table 1. Maximum temperatures and BGE losses for different all-time and time-limited targets.

| | Target X | T_{\max} [°C] | $\Delta BGE_{\text{BAU},X}$ [%] | $\frac{\Delta BGE_{\text{BAU},X}}{\Delta BGE_{\text{BAU},2^\circ\text{C}}}$ |
|-----------------------------------|--------------------------------------|-----------------|---------------------------------|---|
| BAU | | 4.43 | | |
| $T(\forall_t)$ | $\leq 2^\circ\text{C}$ | 2.00 | 0.765 | 1.00 |
| $F(\forall_t)$ | $\leq 815 \text{ GtC}$ | 2.00 | 0.917 | 1.20 |
| $C(\forall_t)$ | $\leq 413 \text{ ppmv}$ | 2.00 | 1.149 | 1.50 |
| A: $C(t \geq 2060)$ | $\leq 413 \text{ ppmv}$ | 2.00 | 0.857 | 1.12 |
| B: $C(t \geq 2160)$ | $\leq 346 \text{ ppmv}$ | 2.00 | 0.934 | 1.22 |
| C: $F(t \leq 2160)$ | $\leq 710 \text{ GtC}$ | 2.00 | 1.340 | 1.75 |
| D: $F(t \leq 2165)$ | $\leq 800 \text{ GtC}$ | 2.00 | 0.965 | 1.26 |
| ECS=2.4°C: $\tilde{F}(\forall_t)$ | $\leq 1000 \text{ GtC}$ | 2.00 | 0.520 | 1.26 |
| $\tilde{C}(t \geq 2100)$ | $\leq 450 \text{ ppmvCO}_2\text{eq}$ | 2.20 | 0.6128 | 0.80 |

Time-limited concentration targets achieve the lowest increase of losses. The lowest observed value is 12% for a time-limited concentration target that peaks at 2°C warming. The strength of time-limited concentration targets originates from their ability to allow for a concentration overshoot. In the appendix we show why a concentration overshoot is compatible with a stable maximum temperature. Higher concentrations allow for more emissions and hence lower losses.

The investigated time-limited cumulative emissions targets did not prove to be sensible. After the targets lose effectivity, emissions and temperatures rise to levels near the BAU scenario. This is not at odds with the time-limited cumulative emissions target by Meinshausen et al. (2009). In their approach, the space of possible scenarios is constrained by further assumptions. However, there is insight from the research on time-limited cumulative emissions targets. The loss structure clearly indicates that early mitigation is most costly. Restricting cumulative emissions further into the future does not cause a considerable further increase of losses.

Lastly, two external targets were investigated. The trillionth tonne target of (Allen et al., 2009) causes an increase of losses of 26% compared to its 2°C parental target when using an ECS of 2.4°C. Stabilizing CO₂eq concentration at 450 ppmvCO₂eq is 20% less costly than the all-time 2°C target but overshoots to 2.2°C.

In conclusion, the time-limited concentration framing and all-time cumulative emissions framing perform best in mimicking the 2°C target. They comply at the lowest cost with the 2°C target. The former through the ability to reproduce the concentration profile of the 2°C target well, the latter because of the already found correlation between all-time cumulative emissions and maximum temperature (Allen et al., 2009). We suggest to the integrated assessment community to use either of them. However, we do warn from the use of all-time concentration targets or time-limited cumulative emissions targets as either very high temperatures occur or a strong increase of losses. To the conclusions of Allen et al. (2009) we can add that also in terms of economic losses the cumulative emissions targets perform well.

When asking whether our two identified “champion subsidiary targets” (time-limited concentration targets as the number one and all-time cumulative emissions target as the number two) were of sufficient accuracy, one would need to judge whether an accuracy of 0.1°C or an economic inaccuracy of 12% (20% for the latter) were acceptable.

Finally, we would like to highlight the caveats of our analysis. The climate and carbon cycle module has limitations and only allows for the proof of principle and order-of-magnitude-estimates. Also our analysis only tackles carbon dioxide emissions (and indirectly sulfur emissions) as control variable, while assuming any other anthropogenic forcing as exogenous. Furthermore, the integrated assessment model utilized does not foresee the option of negative emissions, hence our estimates need to be interpreted as the boundary case of not employing that technology. Additionally, we did not fully explore the range of scenario types already displayed in the literature. In particular we did not calculate peaking-and-decline style of scenarios (den Elzen and van Vuuren, 2007; Meinshausen et al., 2006). Finally we ignored uncertainty. We expect that by proper framing of decision-making under uncertainty within a target-based decision environment, deterministic CEA, like the one presented here, can again (like in Held et al. (2009) and Neubersch et al. (2014)) serve as a good approximation of a full-fledged uncertainty-based analysis.

In spite of these shortcomings we expect to stimulate a discussion on whether the IAM community would need to explicitly calculate temperature targets in the future or whether it can continue living on subsidiary targets as the current standard approach. We have outlined potentially useful concepts, valid orders of magnitude, and crucial candidates for future subsidiary targets, that are not prominent in the community so far (IPCC WGIII, 2014, Ch. 6).

Data availability. Result data is available upon request.

35 **Appendix A: Background: Why do additional constraints cause additional losses?**

Fig. A1 illustrates why additional constraints lead to a welfare loss. The two abscissas represent two dimensions of the control space of the optimization problem and the ordinate represents the value of the goal variable. Without additional constraint, the

optimization is done over the full solution space which is assumed to have no local maxima. Point “A” is the optimal solution in this case. The grey plane represents an additional constraint to the optimization problem, in our case a climate target. Now only points on the intersection of the colored surface and the grey plane are eligible. The new optimum is point “B”. The stricter the target, the more losses are implied. Inverting the argument: once a target is applied, the optimal solution fully exploits the

5 range the target would allow for.

Welfare loss due to a constraint

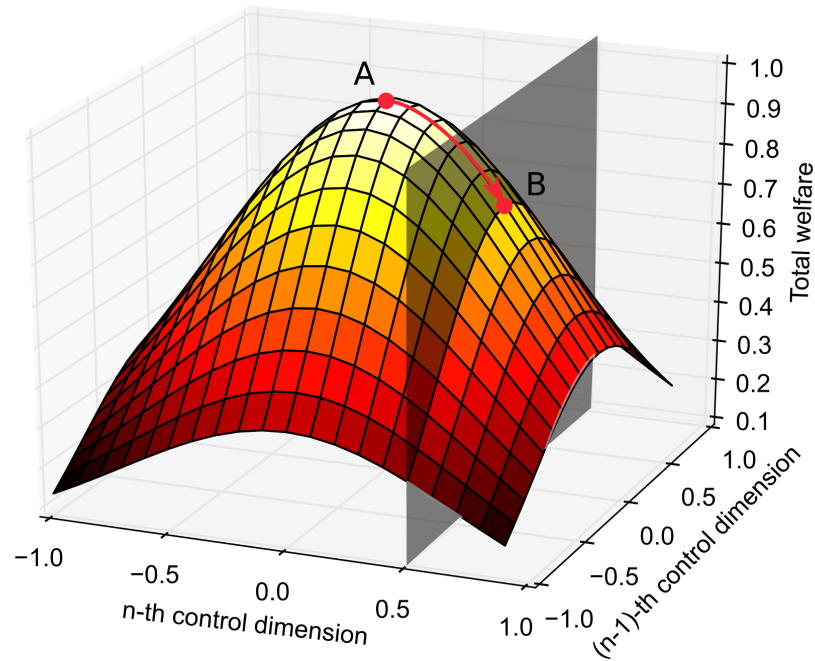


Figure A1. Effective climate targets represent an additional constraint (grey plane) to the welfare of the BAU scenario (colored). The welfare maximum decreases from A to B. Therefore, effective mitigation scenarios always represent losses compared to a baseline scenario without constraints. (Reprinted from Held (2013, Fig. 3))

For completeness: An additional constraint does not necessarily lead to lower welfare, but it does not increase welfare. Welfare therefore either decreases or remains at the same level under an additional constraint.

Appendix B: Application example of climate module

A simple application example of the climate module is shown in Fig. B1, where the initial conditions are taken for the year 2010 from the RCP-database (<http://tntcat.iiasa.ac.at/RcpDb>) for RCP8.5: $E_0 = 9.9$ GtC/a, $F_0 = 450$ GtC, $C_0 = 392$ ppmvCO₂ and $T_0 = 0.95^\circ\text{C}$. Sulfur and OGHG emissions are disregarded in this example. The chosen mitigation scenario reduces GHG emission by 5% yearly. The peak temperature under this assumption is $T \approx 1.5^\circ\text{C}$ and is reached 45 yrs after the simulation start.

10

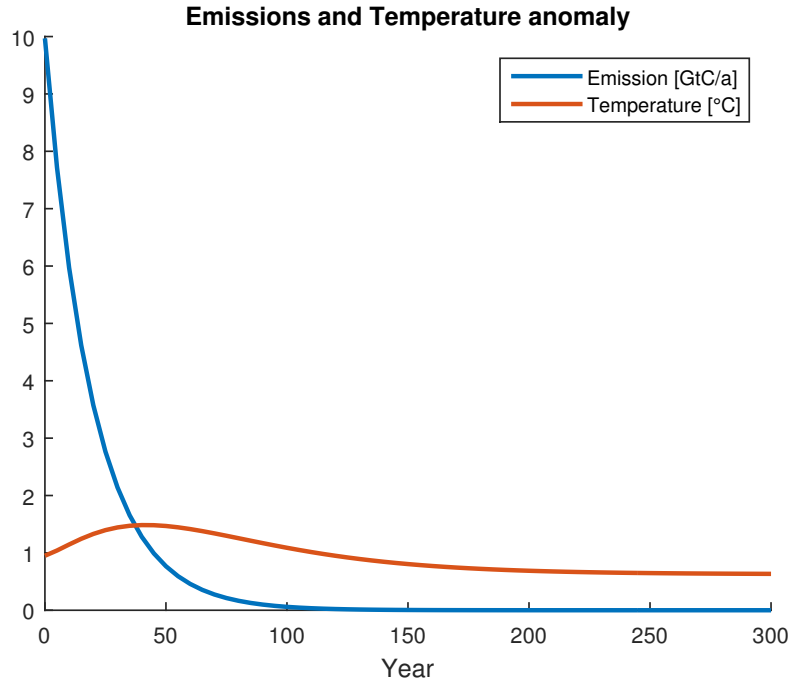


Figure B1. Application example of the climate module. Starting point is 2010 with $E_0 = 9.9$ GtC/a, $F_0 = 450$ GtC, $C_0 = 392$ ppmvCO₂ and $T_0 = 0.95^\circ\text{C}$. Mitigation: 5% emission reductions yearly assuming ECS of 2.8°C .

Appendix C: Conversion of OGHG-forcing into CO₂eq concentration

Why is a conversion necessary?

IPCC WGIII (2014, Chap. 6) stated that many different models have been used to assess possible mitigation or BAU scenarios. Due to the internal differences of these models, namely which GHGs, aerosols they resolve, the model results can not be compared straight forward. Therefore IPCC WGIII (2014) somewhat randomly (for motivation see Chap. 6) decided that the comparison metric is full radiative forcing in 2100 expressed in CO₂eq concentration. In other words, which CO₂ concentration is needed to obtain the same radiative forcing of all agents together. To calculate the radiative forcing and the corresponding CO₂eq concentration, IPCC WGIII (2014) applied MAGICC as published by Meinshausen et al. (2011a).

In MIND only dynamics for CO₂ are implemented. Besides CO₂, OGHG such as CH₄ and N₂O are included as a fixed external forcing vector (Neubersch, 2014). The data originates from the RCP 3P scenario (Van Vuuren et al., 2006) which are implemented via the file oghg_rcp3pd.inc. Aerosols are neglected except for SO₂, which is linearly coupled to the CO₂ emissions and is assumed to decay immediately, *c.f.* Sec. 2.2.1.

Applying MAGICC is complicated and requires a lot of input data but we still want to know the approximate CO₂ concentration that would be needed to express the full radiative forcing through CO₂.

15 How is the conversion done?

MIND calculates radiative forcing of CO₂ as follows:

$$R_{\text{CO}_2} = \ln\left(\frac{C}{C_{\text{pi}}}\right) \frac{R_{2\times\text{CO}_2}}{\ln 2} \quad (\text{C1})$$

where R_{CO_2} is the radiative forcing of CO_2 , $R_{2\times\text{CO}_2}$ the resulting forcing for a doubling of CO_2 concentration, C the actual CO_2 concentration and C_{pi} the preindustrial concentration.

MIND then simply adds R_{OGHG}

$$R_{\text{total}} = R_{\text{CO}_2} + R_{\text{OGHG}} \stackrel{!}{=} \ln\left(\frac{C_{\text{eq}}}{C_{\text{pi}}}\right) \frac{R_{2\times\text{CO}_2}}{\ln 2} \quad (\text{C2})$$

5 which we set equal to a new full radiative forcing of a CO_2 eq concentration of C_{eq} . Solving for C_{eq} gives

$$C_{\text{eq}} = C_{\text{pi}} \cdot \exp\left(\frac{\ln 2 \cdot R_{\text{total}}}{R_{2\times\text{CO}_2}}\right) \quad (\text{C3})$$

$$= C_{\text{pi}} \cdot \exp\left(\frac{\ln 2 \cdot (R_{\text{CO}_2} + R_{\text{OGHG}})}{R_{2\times\text{CO}_2}}\right). \quad (\text{C4})$$

As both R_{CO_2} and R_{OGHG} appear in the exponent is not possible to obtain the pure contribution of OGHG in terms of CO_2 eq concentration, only if the exponential is linearized. As R_{CO_2} and R_{OGHG} are both in the same order of magnitude linearization

10 causes strong errors and is not recommended.

Calculation

Commonly $R_{2\times\text{CO}_2} = 3.7 \text{ W/m}^2$ is used, also MIND. Further, the preindustrial concentration is $C_{\text{pi}} = 280 \text{ ppmvCO}_2$ eq.

$$C_{\text{eq}} = 280 \text{ ppmvCO}_2\text{eq} \cdot \exp\left(\frac{\ln 2 \cdot (R_{\text{CO}_2} + R_{\text{OGHG}})}{3.7 \text{ W/m}^2}\right). \quad (\text{C5})$$

For the 2°C scenario the result and it's numerical decomposition can be seen in Fig. C1. The additional concentration caused by

15 OGHGs in MIND lies approximately between 50 to 90 ppmv. The concentration peak shifts from $C_{2^\circ\text{C}}(2040) = 441.8 \text{ ppmvCO}_2$ to $C_{2^\circ\text{C}}(2035) = 534.5 \text{ ppmvCO}_2$ eq.

Caution

These concentrations should not be used as input for a climate model. The time dynamics will not be reproducible by a modeled carbon cycle because part of the concentration originates from OGHGs and therefore follows different dynamics.

20 Appendix D: A concentration overshoot that is compatible with the 2°C target

A concentration overshoot followed by a stable plateau is compatible with the 2°C target because temperature follows the concentration with a delay. This delayed reaction of the temperature can be used for a concentration overshoot as such that the stable temperature is attained earlier but not transgressed. In the following simple exercise we try to understand this behavior analytically.

25 For simplicity, we assume that the stable concentration for 2°C is already reached, but the temperature is still below 2°C . The temperature then rises towards the stable level of 2°C . Then we allow a concentration overshoot, such that 2°C are reached earlier and more emissions are allowed.

First, the pure CO_2 concentration plateau for 2°C needs to be determined. We extract it from Eq. (3) by neglecting OGHG and SO_2 forcing and by using the parameters of Sec. 2.2.1:

$$30 \quad \dot{T} \stackrel{!}{=} 0 = \mu \ln c - \alpha T = \mu \ln(C/C_{\text{pi}}) - \alpha T \quad (\text{D1})$$

$$\Rightarrow C_{2^\circ\text{C}} = C_{\text{pi}} \exp\left(\frac{\alpha}{\mu} T\right) \approx 460 \text{ ppmv} \quad (\text{D2})$$

$$\Rightarrow c_{2^\circ\text{C}} \approx 1.6429 \quad (\text{D3})$$

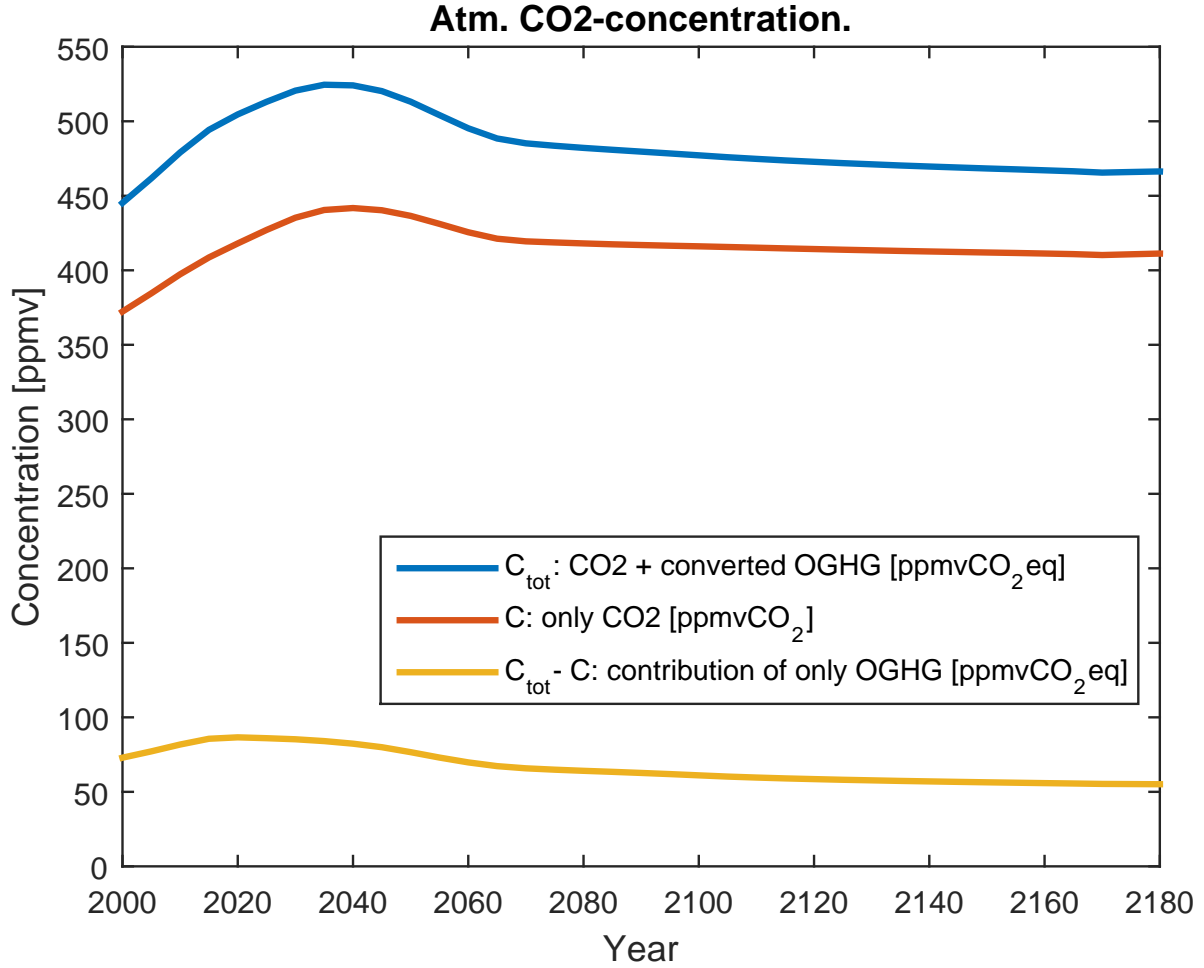


Figure C1. The total C_{eq} concentration was calculated by conversion of the total radiative forcing into equivalent CO₂ concentration (blue). The red curve shows the actual CO₂ concentration in the model caused by fossil burning and land use change. The yellow line shows the difference. The data originates from the 2°C mitigation scenario.

Note that capital C stands for the absolute concentration in ppmv and not for the anomaly as in Sec. 2.2.1. However, c stands for the ratio to C_{pi} and is equal to the c in Sec. 2.2.1. The conversion between C and c is $c \cdot 280\text{ppmv} = C$. In the following we use the ratio to pre-industrial concentration c without unit.

Hence, the baseline concentration is $c_{2^\circ\text{C}}$. We now determine the temperature rise caused by this stable concentration, where we use the 1995 temperature, $T_0 = 0.9488^\circ\text{C}$, of MIND as an initial condition. Out of convenience the year 1995 is identified with $t = 0$.

Before solving Eq. (3) we perform a first order Taylor expansion on the logarithm around $c_{2^\circ\text{C}}$. This gives:

$$\ln c \approx \ln c_{2^\circ\text{C}} + \frac{c}{c_{2^\circ\text{C}}} - 1 + \mathcal{O}(c^2). \quad (\text{D4})$$

Using this approximation, $c = c_{2^\circ\text{C}}$ and $T(0) = T_0$, we get a temperature that asymptotically approaches 2°C:

$$T(t) = e^{-\alpha t} \left(T_0 + \frac{\mu}{\alpha} (e^{\alpha t} - 1) \ln c_{2^\circ\text{C}} \right). \quad (\text{D5})$$

The function is plotted in Fig. D1 using the parameters given in Sec. 2.2.1.

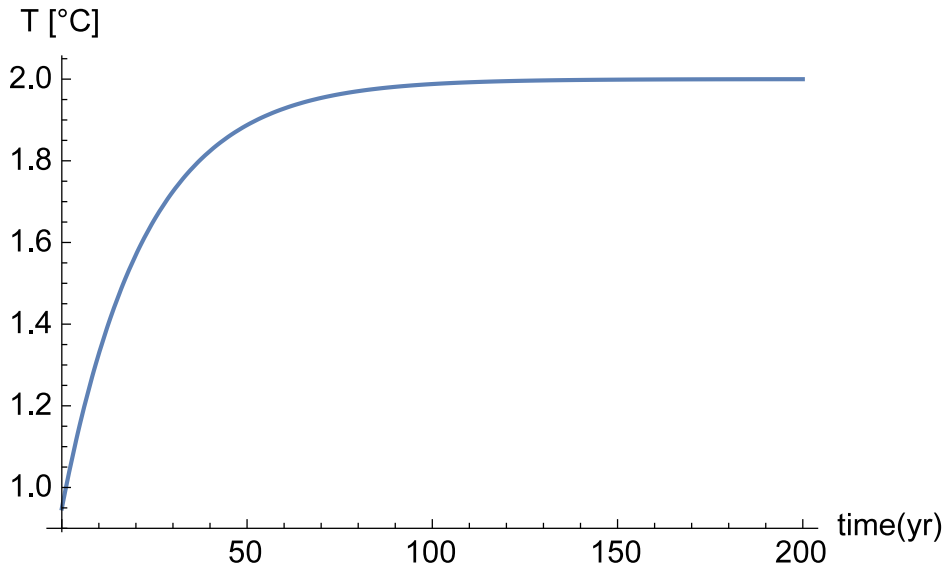


Figure D1. The resulting temperature starting at $T_0 = 0.9488^\circ\text{C}$ under a constant concentration forcing of $c_2^\circ\text{C}$.

The overshoot is modeled using a parabola. The parabola has a width t_w , a peak-time t_p and peak height c_p . The overshoot concentration $\hat{c}(t)$ is shown in Fig. D2 and reads:

$$\hat{c}(t) = \begin{cases} c_p - \frac{c_p(t-t_p)^2}{t_w^2} & t_p - t_w < t < t_p + t_w \\ 0 & \text{else} \end{cases} \quad (\text{D6})$$

As we have linearized the logarithm in Eq. (3) we can use the superposition principle and solve Eq. (3) for the parabolic overshoot individually. The solutions can then be added later.

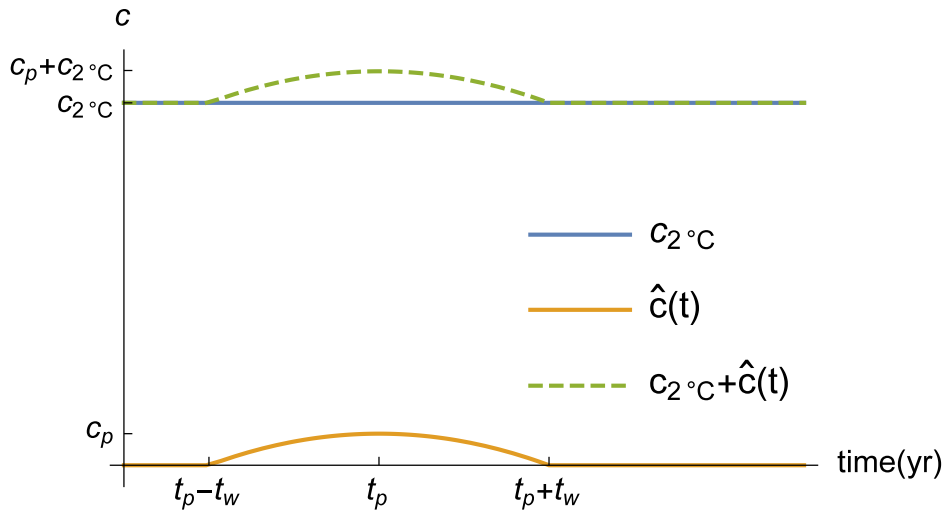


Figure D2. The concentration forcing for the all-time concentration target (blue), the overshoot concentration (orange) and the sum of both (green).

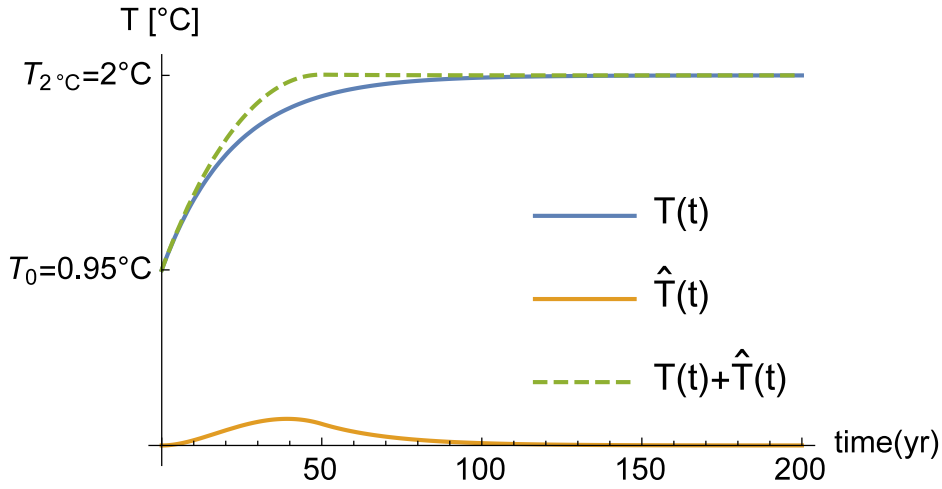


Figure D3. Temperature responses for the concentration forcing $c_{2^\circ\text{C}}$, $\hat{c}(t)$ and $c_{2^\circ\text{C}} + \hat{c}(t)$ using the parameters given in the text.

We solve Eq. (3) for $\hat{c}(t + t_p)$ as a deviation from the steady state $c_{2^\circ\text{C}}$. Note that the concentration signal was shifted to be symmetric around zero. The temperature result has to be shifted back. The start condition here is the steady state $T(-t_w) = T_{2^\circ\text{C}} = 2^\circ\text{C}$. From the solution we subtract $T_{2^\circ\text{C}}$ again in order to obtain the pure deviation from the steady state. If we additionally use the fact that $T_{2^\circ\text{C}} = \frac{\mu}{\alpha} \ln(c_{2^\circ\text{C}})$, the solution reads:

$$5 \quad \hat{T}(t) = \begin{cases} 0 & t < -t_w \\ \frac{1}{\alpha^2 t_w^2} \frac{c_p}{c_{2^\circ\text{C}}} \frac{\mu}{\alpha} e^{-\alpha(t+t_w)} \left(\underbrace{2\alpha t_w + 2}_a + \underbrace{2e^{\alpha(t+t_w)} (\alpha t - 1 + \alpha^2 t_w^2 - \alpha^2 t^2)}_{b(t)} \right) & -t_w < t < t_w \\ \frac{1}{\alpha^2 t_w^2} \frac{c_p}{c_{2^\circ\text{C}}} \frac{\mu}{\alpha} e^{-\alpha(t+t_w)} \left(\underbrace{2\alpha t_w + 2}_a + \underbrace{2e^{2\alpha t_w} (\alpha t_w - 1)}_{b(t_w)} \right) & t > t_w \end{cases} \quad (\text{D7})$$

Note that for $-t_w < t < t_w$, the function consists out of a pure exponential decay of the factor a , combined with a quadratic function $b(t)$. Factor $b(t)$ is purely quadratic in time because the exponential terms cancel out. For times $t > t_w$ we recognize a again. $b(t)$ is now constant $b(t_w)$ and decays with the same factor as a .

For concrete results, the shape of the overshoot parabola needs to be determined. We assume that the width of the parabola is equal to its peak time, $t_w = t_p$, this means the overshoot starts at $t = 0$. We use $t_w = t_p = 25$ yr and $C_p = 24$ ppmv. The values were designed to not overshoot 2°C . However, this is not the only parameter set that fulfills this criteria and the choice is only for illustration. In future works, it would be nice to determine the shape of the overshoot parabola based on the temperature gap towards 2°C .

Fig. D3 shows both the results of $T(t)$ (blue), $\hat{T}(t)$ (orange) and their superposition $T(t) + \hat{T}(t)$ (green). The $T(t) + \hat{T}(t)$ stays below 2°C but reaches the 2°C level about 50 years earlier. The rise of $T(t)$ and the decay of $\hat{T}(t)$ balance out.

We found an analytical explanation why a concentration overshoot is compatible with staying below 2°C .

References

- Allen, M. R., Frame, D. J., Huntingford, C., Jones, C. D., Lowe, J. A., Meinshausen, M., and Meinshausen, N.: Warming caused by cumulative carbon emissions towards the trillionth tonne, *Nature* 458, 1163, <https://doi.org/doi:10.1038/nature08019>, 2009.
- Anthoff, D. and Tol, R. S.: The impact of climate change on the balanced growth equivalent: An application of FUND, *Environmental and Resource Economics*, 43, 351–367, 2009.
- COP21: Paris Agreement, http://unfccc.int/files/essential_background/convention/application/pdf/english_paris_agreement.pdf, downloaded 9 March 2017, 2015.
- den Elzen, M. G. and van Vuuren, D. P.: Peaking profiles for achieving long-term temperature targets with more likelihood at lower costs, *Proceedings of the National Academy of Sciences*, 104, 17931–17936, 2007.
- Edenhofer, O., Bauer, N., and Kriegler, E.: The impact of technological change on climate protection and welfare: Insights from the model MIND, *Ecological Economics*, 54, 277–292, 2005.
- Hasselmann, K., Hasselmann, S., Giering, R., Ocana, V., and Storch, H.: Sensitivity study of optimal CO₂ emission paths using a simplified structural integrated assessment model (SIAM), *Climatic Change*, 37, 345–386, 1997.
- Held, H.: Climate policy options and the transformation of the energy system, in: L. Cifarelli, F. Wagner, D. S. Wiersma (Eds.): *New Strategies for Energy Generation, Conversion and Storage*, pp. 13–28, Lecture Notes Joint EPS-SIF International School on Energy, Course 1, 30 July – 4 August 2012, Villa Monastero, Varenna, Lake Como, European Physical Society, Società Italiana di Fisica, 2013.
- Held, H., Kriegler, E., Lessmann, K., and Edenhofer, O.: Efficient climate policies under technology and climate uncertainty, *Energy Economics*, 31, S50–S61, 2009.
- IPCC WGI: *Climate Change 2013: The Physical Science Basis. Contribution of Working Group I to the Fifth Assessment Report of the Intergovernmental Panel on Climate Change*, [Stocker, T.F., D. Qin, G. - K. Plattner, M. Tignor, S.K. Allen, J. Boschung, A. Nauels, Y. Xia, V. Bex and P.M. Midgley (eds.)]. Cambridge University Press, Cambridge, United Kingdom and New York, NY, USA, 2013.
- IPCC WGIII: *Climate Change 2014: Mitigation of Climate Change. Contribution of Working Group III to the Fifth Assessment Report of the Intergovernmental Panel on Climate Change*, [Edenhofer, O., R. Pichs-Madruga, Y. Sokona, E. Farahani, S. Kadner, K. Seyboth, A. Adler, I. Baum, S. Brunner, P. Eickemeier, B. Kriemann, J. Savolainen, S. Schlömer, C. von Stechow, T. Zwicker and J.C. Minx (eds.)]. Cambridge University Press, Cambridge, United Kingdom and New York, NY, USA, 2014.
- Khabbazan, M. M. and Held, H.: On the Future Role of the most Parsimonious Climate Module in Integrated Assessment, *Earth System Dynamics Discussions*, 2017.
- Kriegler, E. and Bruckner, T.: Sensitivity analysis of emissions corridors for the 21st century, *Climatic change*, 66, 345–387, 2004.
- Lorenz, A., Schmidt, M. G., Kriegler, E., and Held, H.: Anticipating climate threshold damages, *Environmental Modeling & Assessment*, 17, 163–175, 2012.
- Meinshausen, M., Hare, B., Wigley, T. M., Van Vuuren, D., Den Elzen, M. G., and Swart, R.: Multi-gas emissions pathways to meet climate targets, *Climatic change*, 75, 151–194, 2006.
- Meinshausen, M., Meinshausen, N., Hare, W., Raper, S. C., Frieler, K., Knutti, R., Frame, D. J., and Allen, M. R.: Greenhouse-gas emission targets for limiting global warming to 2 C, *Nature*, 458, 1158–1162, 2009.
- Meinshausen, M., Raper, S., and Wigley, T.: Emulating coupled atmosphere-ocean and carbon cycle models with a simpler model, *MAGICC6–Part 1: Model description and calibration, Atmospheric Chemistry and Physics*, 11, 1417–1456, 2011a.
- Meinshausen, M., Smith, S. J., Calvin, K., Daniel, J. S., Kainuma, M., Lamarque, J., Matsumoto, K., Montzka, S., Raper, S., Riahi, K., et al.: The RCP greenhouse gas concentrations and their extensions from 1765 to 2300, *Climatic change*, 109, 213–241, 2011b.
- Mirrlees, J. A. and Stern, N. H.: Fairly good plans, *Journal of Economic Theory*, 4, 268–288, 1972.
- Neubersch, D.: Value of information under climate targets: an application of cost-risk analysis, Ph.D. thesis, Universität Hamburg Hamburg, 2014.
- Neubersch, D., Held, H., and Otto, A.: Operationalizing climate targets under learning: An application of cost-risk analysis, *Climatic change*, 126, 305–318, 2014.

- Nordhaus, W. D.: *Managing the global commons: the economics of climate change*, vol. 31, MIT press Cambridge, MA, 1994.
- Petschel-Held, G., Schellnhuber, H.-J., Bruckner, T., Toth, F. L., and Hasselmann, K.: The tolerable windows approach: theoretical and methodological foundations, *Climatic Change*, 41, 303–331, 1999.
- Roth, R., Neubersch, D., and Held, H.: Evaluating Delayed Climate Policy by Cost-Risk Analysis, EAERE2015 article, 2015.
- 5 Schneider, S. H. and Mastrandrea, M. D.: Probabilistic assessment of “dangerous” climate change and emissions pathways, *Proceedings of the National Academy of Sciences of the United States of America*, 102, 15 728–15 735, 2005.
- Swart, R., Mitchell, J., Morita, T., and Raper, S.: Stabilisation scenarios for climate impact assessment, *Global Environmental Change*, 12, 155–165, 2002.
- United Nations: U.N. Framework Convention on Climate Change, Earth Summit Rio de Janeiro, 1992.
- 10 Van Vuuren, D., Den Elzen, M., Lucas, P. L., Eickhout, B., Strengers, B., van Ruijven, B., Berk, M., de Vries, H., Hoogwijk, M., Meinshausen, M., et al.: Stabilising greenhouse gas concentrations at low levels: an assessment of options and costs, Netherlands Environmental Assessment Agency, Bilthoven, 2006.
- Van Vuuren, D. P., Den Elzen, M., Berk, M., Lucas, P., Eickhout, B., Eerens, H., and Oostenrijk, R.: Regional costs and benefits of alternative post-Kyoto climate regimes: comparison of variants of the Multi-stage and Per Capita Convergence regimes, 2003.
- 15 WGBU: *World in transition: Towards sustainable energy systems*, vol. 3, Earthscan, wissenschaftlicher Beirat der Bundesregierung Globale Umweltveränderungen (Germany), 2004.